

DESY 78/53
October 1978



WEAK DECAYS OF CHARMED BARYONS

by

J. G. Körner and G. Kramer

II. Institut für Theoretische Physik der Universität Hamburg

J. Willrodt

Deutsches Elektronen-Synchrotron DESY, Hamburg

To be sure that your preprints are promptly included in the
HIGH ENERGY PHYSICS INDEX,
send them to the following address (if possible by air mail) :

DESY
Bibliothek
Notkestrasse 85
2 Hamburg 52
Germany

Weak Decays of Charmed Baryons

J. G. Körner and G. Kramer

II. Institut für Theoretische Physik der Universität Hamburg

J. Willrodt ⁺)

Deutsches Elektronen-Synchrotron DESY, Hamburg

Abstract

We use the quark model framework to calculate the weak decays of the lowest lying charmed baryons into ground state baryons and mesons. We present detailed results on the predicted flavour and multipole composition of the final state configurations which can be tested in the near future. For the decays $1/2^+ \rightarrow 1/2^+ + 0^-$ we also give symmetry and current algebra estimates which we compare with the quark model results. Semileptonic branching ratios in charmed baryon decays are calculated to be of the order of $\sim 5\%$. The total lifetime of charmed baryons is predicted to be $\sim 7 \times 10^{-14}$ sec which is 5 - 10 times smaller than the free quark model estimate.

⁺) On leave of absence from Gesamthochschule Siegen

1. Introduction

In a recent e^+e^- annihilation experiment at SPEAR [1,2] the inclusive production of baryons showed a marked increase when the beam energy was raised through the expected threshold for charmed baryon pair production at $\sqrt{s} \sim 4.5$ GeV. It is believed that this is the long expected signal for charmed baryon pair production in e^+e^- -annihilation. Previously charmed baryon candidates have been identified in a neutrino production [3] and in a photoproduction experiment [4].

The interpretation of charmed meson decays has been successfully guided by the GIM scheme [5]. Similarly one expects the decay products of the lowest charmed baryon to dominantly contain a strange quark. Recently the issue was raised whether the s-quark from c-decay turns up in the final state baryon or in the final state mesons since the small yield of excess Λ 's (or $\bar{\Lambda}$'s) compared to excess \bar{p} 's above charmed baryon threshold is somewhat puzzling [1].

In a previous note we have addressed ourselves to the above problem by calculating C_0^+ (cud) decays in a quark model [6]. In this paper we present details of the calculation as well as extending the calculation to include the weak decays of the next stable charmed baryons $A^{+,0}$ (csu(d)) and T^0 (css) decays.

We take the point of view that the lowest charmed baryons decay into two body and quasi two body states most of the time. This is orthogonal to a statistical description of these decays [7] in which multiple mesons originat-

ing from weak charmed baryon decays are essentially uncorrelated except for possible jet configurations. The latter approach already seems to be at variance with some of the observed D-decay modes [8]. On the other hand resonance dominance of multibody final states in most production processes has been firmly established in the last few years.

We shall be mainly concerned with the Cabibbo favoured decays of the lowest charmed baryons into ground state mesons and baryons. The bulk of the lowest charmed baryons decays should consist of these channels. Higher resonance contributions are suppressed because of phase space, and, in the case of higher baryon resonances, due to a dynamic suppression caused by the suppressed quark model wave function overlap between ground state and excited state baryons. Cabibbo suppressed decays to the low lying baryons and mesons are not likely to be important due to the Cabibbo suppression factor $\text{tg}^2 \Theta_c \sim 5\%$.

The plan of the paper is the following. In sec. 2 we discuss the structure of the effective current x current charm changing Hamiltonian that arises from the operator product expansion of the product of free quark currents at short distances [9]. We systematically discuss a number of sum rules that arise from the flavour symmetry properties of the effective Hamiltonian using various subgroups of SU(4). These sum rules relate charm changing decays among each other as well as $\Delta C = 1$ decays to the $\Delta C = 0$ hyperon decays. Sec. 2 also contains a discussion of the spectrum of charmed baryons. In sec. 3 we present the details of the quark model calculation and give our results on partial rates, total rates, asymmetry parameters, charged multiplicities, inclusive rates and semileptonic branching ratios. Where possible we compare the quark model results with the results of calculating the decay

amplitudes from SU(4) using the known $\Delta C = 0$ nonleptonic hyperon decay data as input. Since the calculated quark model amplitudes incorporate symmetry breaking effects we discuss how the sum rules derived in sec. 2 may be affected by symmetry breaking. Sec. 4 contains the results of a current algebra evaluation of some of the transition amplitudes. In sec. 5 we give a summary of our results. Technical details are relegated to the appendices. Appendix A contains the calculation of the factorizing contributions. In appendix B we present a proof of the identity of the tensor invariants describing the parity violating (p.v.) amplitude in the process $1/2^+ \rightarrow 1/2^+ + 0^-$ using current algebra plus soft pion techniques on the one hand and quark model diagrams on the other hand. Appendix C finally contains some kinematic definitions and rate formulae needed for the discussion in the main text.

II. Symmetry Relations

The ground state charmed baryons are classified as usual as members of the (inequivalent) SU(4) multiplets $20'$ and 20 . The $J = 1/2$ ground state baryons (containing the ordinary $C = 0$ octet baryons) comprise the $20'$ representation and the $J = 3/2$ ground state baryons (containing the ordinary $C = 0$ decuplet baryons) comprise the 20 representation. In tables 1 and 2 we have listed the quantum number content of the charmed baryon members of the $20'$ and 20 , where we have used the same notation as in [10].

The mass values in tables 1 and 2 are estimated by the methods of [11], where we have used $M_{C^+} = 2.26$ GeV and recent values for the D , D^* , F and F^* masses as input. If these mass estimates are correct then the baryon

states C_0^+ , A^+ , A^0 , T^0 , X_u^{++} , X_d^+ , X_s^+ and Θ^{++} must decay weakly. In this paper we shall only be concerned with the lower mass $C = 1$ charmed baryons C_0^+ , A^+ , A^0 and T^0 leaving the discussion of the $C = 2$ and $C = 3$ baryons for future investigations.

A discussion of charm changing weak decays proceeds from the interaction Hamiltonian

$$\mathcal{H} = g_w^2 \int d^4x D_F(x, m_w^2) T(\mathcal{J}_\mu^{\Delta c}(x) \mathcal{J}^\mu(0)) + h.c. \quad (2.1)$$

where g_w is the weak gauge coupling constant and D_F is the W -boson propagator.

$\mathcal{J}_\mu^{\Delta c}$ and \mathcal{J}_μ are the charm changing and charm conserving charged GIM currents [5]

$$\mathcal{J}_\mu^{\Delta c} = \bar{c} \gamma_\mu (1 - i\gamma_5) (\cos \theta_c s - \sin \theta_c d) \quad (2.2)$$

and

$$\mathcal{J}_\mu = \bar{u} \gamma_\mu (1 - i\gamma_5) (\cos \theta_c d + \sin \theta_c s) \quad (2.3)$$

where a summation over colour indices is implied in (2.2) and (2.3).

The dominant piece in (2.1) is proportional to $\cos^2 \theta_c$ and obeys the selection rule $\Delta C = \Delta S = \Delta I = 1$. The selection rules for the Cabibbo suppressed parts in (2.1) proportional to $\cos \theta_c \sin \theta_c$ and $\sin^2 \theta_c$ are given in table 3. Since the corresponding modes are suppressed by factors $\tan^2 \theta_c$ and $\tan^4 \theta_c$ we shall, however, discuss only Cabibbo favoured decays in the following.

From a reduction of the current product in (2.1) one finds that the Hamiltonian (2.1) can be split up into two pieces transforming as $20''$ and 84 in $SU(4)$. Let us define two corresponding operators \mathcal{O}^- and \mathcal{O}^+ with the above $SU(4)$ transformation properties by writing

$$\mathcal{O}^\mp = \left((\bar{s}c)_L (\bar{u}d)_L \mp (\bar{s}d)_L (\bar{u}c)_L \right) \quad (2.4)$$

In (2.4) we have employed the short hand notation $(\bar{s}c)_L = \bar{s} \gamma_\mu (1 - i\gamma_5) c$ etc.

The Hamiltonian (2.1) can be seen to be dominated by the short distance properties of the current x current product [12] which can be calculated in an asymptotically free theory as in QCD [9]. The resulting interaction Hamiltonian is then well approximated by an effective local form

$$\begin{aligned} \mathcal{H}_{\text{eff.}} &= \frac{G}{\sqrt{2}} \cos^2 \Theta_c (f_- \mathcal{O}^- + f_+ \mathcal{O}^+) \\ &\equiv \mathcal{H}_{\text{eff.}}^{20''} + \mathcal{H}_{\text{eff.}}^{84} \end{aligned} \quad (2.5)$$

where the coefficients f_- and f_+ in (2.5) can be estimated from calculating the hard gluon contributions to (2.1). One obtains $f_- > 1 > f_+$ which means that the $20''$ contribution in (2.5) dominates over the 84 contribution [13].

The considerations in this section are not dependent on the exact numerical values of f_- and f_+ in (2.5), since we shall be writing down separate sum-rules for the two pieces in the effective Hamiltonian (2.5). Independent of the numerical values of f_\pm calculated in [13,14,15,16] the relative importance of the two pieces in (2.5) may perhaps eventually be judged by how well the

two respective sets of sum rules are satisfied.

Most of the sum rules for charmed baryon decays following from (2.5) do not in fact require full use of the SU(4) or SU(3) properties of (2.5), but a consideration of the SU(2) I, U and V spin subgroups will suffice. Using the relevant raising operators

$$\begin{array}{lll}
 I_+ d = u & U_+ s = d & V_+ s = u \\
 I_+ \bar{u} = -\bar{d} & U_+ \bar{d} = -\bar{s} & V_+ \bar{u} = -\bar{s}
 \end{array} \tag{2.6}$$

one readily sees that \mathcal{H}_{eff} (2.5) transforms as a U- and I-spin vector whereas \mathcal{H}_{eff} is in general a mixture of the two V spin operators, since $\mathbf{0}^-$ and $\mathbf{0}^+$ transform as V-spin scalars and vectors, respectively. In tables 4a, 4b and 4c we have listed the relevant I, U and V spin multiplets for the mesons and baryons of interest, where we use the phase convention $I_{\pm} |I, I_3\rangle = ((I \pm I_3)(I \mp I_3 + 1))^{1/2} |I, I_3 \pm 1\rangle$, and similarly for U_{\pm} and V_{\pm} . The sum rules given in tables 5a-5d can then simply be worked out by using SU(2) Clebsch-Gordan tables. Since we are employing quark model phase conventions in our later calculations we have changed some of the phases in 5a-5d in order to present one consistent set of phases. Note that the sum rules are not all linearly independent. As pointed out in [17] one can also derive a number of interesting sum rules for the total and partial decay rates of C_0^+ and A^0 if one keeps only the $\mathbf{20}''$ piece in \mathcal{H}_{eff} . Since $\mathcal{H}_{\text{eff}}^{\mathbf{20}''}$ is a V-spin scalar and C_0^+ and A^0 are members of the same V-spin doublet (see table 4b) one can easily show that C_0^+ and A^0 must have the same total rate as well as the same rates into particular spin configurations. Thus one obtains

$$\Gamma_{\text{total}}(C_0^+) = \Gamma_{\text{total}}(A^0) \quad (2.7)$$

$$\sum_{i,j} \Gamma(C_0^+ \rightarrow B_i + M_j) = \sum_{i,j} \Gamma(A^0 \rightarrow B_i + M_j) \quad (2.8)$$

where the B_j are either the $1/2^+$ or $3/2^+$ baryons and the M_j the 0^- or 1^- mesons. In the case of transitions to the $J = 1/2$ ground state baryons there are further sum rules. The derivation of these, however, require the use of the full SU(3) -uds- properties of the \mathcal{O}^+ in \mathcal{H}_{eff} . First, there is one sum rule which holds for a general linear combination of \mathcal{O}^+ and \mathcal{O} :

$$\begin{aligned} \sqrt{3} \left((C_0^+ \rightarrow \Sigma^+ \eta_8) - (C_0^+ \rightarrow \Lambda \pi^+) \right) &= -\sqrt{2} \left((A^0 \rightarrow \Xi^- \pi^+) - (A^0 \rightarrow \Sigma^+ K^-) \right) \\ &\quad - (A^0 \rightarrow \Xi^0 \pi^0) + \sqrt{3} (A^0 \rightarrow \Xi^0 \eta_8) \end{aligned} \quad (2.9)$$

Second, from the SU(4) transformation property of $\mathcal{H}_{\text{eff}}^{20''}$ and $\mathcal{H}_{\text{eff}}^{84}$ one has the two following set of sum rules

$\mathcal{H}_{\text{eff}}^{20''}$

$$(C_0^+ \rightarrow \Lambda \pi^+)_{\text{p.v.}} = 0$$

$$\sqrt{3} (C_0^+ \rightarrow p \bar{K}^0)_{\text{p.v.}} + \sqrt{2} (A^0 \rightarrow \Lambda \bar{K}^0)_{\text{p.v.}} = 0$$

$$\sqrt{6} (C_0^+ \rightarrow p \bar{K}^0)_{\text{p.v.}} - \sqrt{6} (C_0^+ \rightarrow \Xi^0 K^+)_{\text{p.v.}} - (T^0 \rightarrow \Xi^0 \bar{K}^0)_{\text{p.v.}} = 0 \quad (2.10)$$

$$\sqrt{2} (C_0^+ \rightarrow \Lambda \pi^+)_{\text{p.c.}} - \sqrt{3} (C_0^+ \rightarrow p \bar{K}^0)_{\text{p.c.}} - \sqrt{2} (A^0 \rightarrow \Lambda \bar{K}^0)_{\text{p.c.}} = 0$$

$\mathcal{X}_{\text{eff.}}^{84}$

$$\begin{aligned} (C_0^+ \rightarrow \Lambda \pi^+)_{\text{p.v.}} &= 0 \\ (C_0^+ \rightarrow \rho \bar{K}^0)_{\text{p.v.}} + 2(C_0^+ \rightarrow \Xi^0 K^+)_{\text{p.v.}} + \sqrt{6}(A^0 \rightarrow \Lambda \bar{K}^0)_{\text{p.v.}} &= 0 \end{aligned} \quad (2.11)$$

The derivation of the sum rules (2.10) and (2.11) requires in addition use of the charge conjugation properties of $\mathcal{X}_{\text{eff.}}$ which from CP invariance is $C = -1$ for p.v. amplitudes and $C = +1$ for p.c. amplitudes. It is noteworthy that $(C_0^+ \rightarrow \Lambda \pi^+)_{\text{p.v.}} = 0$ for any linear combination of $\mathcal{X}_{\text{eff.}}^{20''}$ and $\mathcal{X}_{\text{eff.}}^{84}$ (see also [18]).

In tables 4a and 5a-5d and in (2.9) the states η_8 and η_{15} refer to the unphysical $I = 0$ η -state transforming as the SU(3) octet and singlet members of the 15-dimensional SU(4) representation [19] ($\eta_8 = (u\bar{u} + d\bar{d} - 2s\bar{s})/\sqrt{6}$; $\eta_{15} = (u\bar{u} + d\bar{d} + s\bar{s} - 3c\bar{c})/\sqrt{12}$).

The physical η and η' states are empirically well approximated by the so called Isgur's wavefunctions

$$\begin{aligned} \eta &= (u\bar{u} + d\bar{d} - \sqrt{2}s\bar{s})/2 \\ \eta' &= (u\bar{u} + d\bar{d} + \sqrt{2}s\bar{s})/2 \end{aligned} \quad (2.12)$$

which means that η_8 is a linear superposition of η and η' given by

$$\eta_8 = (6)^{-1/2} ((1+\sqrt{2})\eta + (1-\sqrt{2})\eta') \quad (2.13)$$

Since (2.13) shows that $\eta \sim \eta_8$ the sum rules involving η_8 may in some cases be valid also for the η depending on the coupling strength of the η' .

In order to obtain relations involving the η' one would need information about transitions to the SU(4) singlet state η_8 . Since this is lacking we cannot make any symmetry predictions involving the η' .

It is clear that the relations in table 5a-5d as well as the sumrule (2.9) are also applicable to transitions involving vector mesons if the appropriate changes in notation are made. The isoscalar octet state is now given by

$$\omega_8 = (1/3)^{1/2} \omega - (2/3)^{1/2} \varphi \quad (2.14)$$

where we have assumed ω and φ to be ideally mixed.

In order to be able to assess the completeness of the sum rules derived so far one has to count the number of SU(4) invariants describing the relevant transitions. This can best be done by counting the CP and SU(4) invariant couplings in the t-channel $B + \bar{B} \rightarrow M$.

For the $1/2^+ \rightarrow 1/2^+ + 0^-$ case one needs the following decompositions

$$\begin{aligned} 20' \otimes \bar{20}' &= 1^{(+)} + 15_1^{(+)} + 15_2^{(+)} + 20''^{(-)} + 45^{(-)} + \bar{45}^{(-)} + 84^{(-)} + 175^{(+)} \\ 20'' \otimes 15 &= 15 + 20'' + 45 + \bar{45} + 175 \\ 84 \otimes 15 &= 15 + 45 + \bar{45} + 84_1 + 84_2 + 175 + 256 + \bar{256} + 300 \end{aligned} \quad (2.15)$$

where we have indicated the symmetry nature of the reduced representations in $20' \otimes \bar{20}'$ by a superscript. Then one has for the two cases $\mathcal{X}_{\text{eff}}^{20''}$ and $\mathcal{X}_{\text{eff}}^{84}$ the following t-channel reduced matrix elements

(i) $\mathcal{R}_{\text{eff.}}^{20''}$

$$\text{p.v. amplitude} \quad R_{20''}^t ; R_{45+45}^t \quad (2.16)$$

$$\text{p.c. amplitude} \quad R_{15_1}^t ; R_{15_2}^t ; R_{45-45}^t ; R_{175}^t$$

(ii) $\mathcal{R}_{\text{eff.}}^{84}$

$$\text{p.v. amplitude} \quad R_{45+45}^t ; R_{84_1}^t ; R_{84_2}^t \quad (2.17)$$

$$\text{p.c. amplitude} \quad R_{15_1}^t ; R_{15_2}^t ; R_{45-45}^t ; R_{175}^t$$

Adding the number of sum rules in table 5a, 5b and 5c to those in (2.9) and (2.10) derived from $\mathcal{R}_{\text{eff.}}^{20''}$ one has 17 relations for 15 s-wave amplitudes and 15 relations for the 15 p-wave amplitudes. Judging from (2.16) this shows that the sum rules are not all linearly independent.

For $\mathcal{R}_{\text{eff.}}^{84}$ one finds correspondingly 15 relations for the 15 p.v. amplitudes and 13 relations for the 15 p.c. amplitudes. Again the sum rules are not linearly independent as can be judged from (2.17).

For the processes $1/2^+ \rightarrow 3/2^+ + 0^-$ one needs the decomposition

$$20 \otimes \overline{20}' = 15 + 45 + 84 + 256 \quad (2.18)$$

Thus one has the two invariants R_{15}^t and R_{45}^t for $\mathcal{R}_{\text{eff.}}^{20''}$ and the five invariants R_{15}^t , R_{45}^t , $R_{84_1}^t$, $R_{84_2}^t$ and R_{256}^t for $\mathcal{R}_{\text{eff.}}^{84}$. In this case there are no additional relations from CP invariance.

The sum rules (2.10) and

(2.11) which only follow from the complete SU(4) transformation properties of $\mathcal{X}_{\text{eff.}}^{20''}$ and $\mathcal{X}_{\text{eff.}}^{84}$ can be derived using SU(4) Clebsch-Gordan tables [20]. Another way of deriving these is to use the tensor method first applied to SU(4) by Iwasaki [21]. Here the 20'' and 84 pieces of $\mathcal{X}_{\text{eff.}}$ are represented by the traceless antisymmetric tensors $T_{[c d]}^{[a b]}$ and the traceless symmetric tensor $T_{\{c d\}}^{\{a b\}}$, respectively. In the following we shall discuss only applications involving the antisymmetric part of $\mathcal{X}_{\text{eff.}}$.

The transition $1/2^+ \rightarrow 1/2^+ + 0^-$ is now represented by the following SU(4) tensor invariants

$$\begin{aligned}
 T_{\text{p.c.}}^{\text{p.v.}} = & a \bar{F} \left(H_{[ke]}^{[ij]} \bar{B}_{[nm]}^k B_i^{[ne]} M_j^m + H_{[ij]}^{[ke]} \bar{B}_{[ne]}^i B_k^{[nm]} M_m^j \right) \\
 & + b \bar{F} \left(H_{[ke]}^{[ij]} \bar{B}_{[im]}^n B_j^{[km]} M_n^e + H_{[ij]}^{[ke]} \bar{B}_{[km]}^j B_n^{[im]} M_e^n \right) \\
 & + c \bar{F} \left(H_{[ke]}^{[ij]} \bar{B}_{[ij]}^e B_m^{[kn]} M_n^m + H_{[ij]}^{[ke]} \bar{B}_{[kn]}^m B_e^{[ij]} M_m^n \right) \\
 & + d \bar{F} \left(H_{[ke]}^{[ij]} \bar{B}_{[ij]}^m B_m^{[kn]} M_n^e + H_{[ij]}^{[ke]} \bar{B}_{[kn]}^m B_m^{[ij]} M_e^n \right)
 \end{aligned} \tag{2.19}$$

where one has incorporated the correct C-conjugation behaviour. The $B_i^{[j k]}$ and M_i^j are baryon and meson tensors transforming as 20' and 15 in SU(4) and are given in [22].

It turns out to be much more convenient to use a different representation for the baryon tensors

$$B_i^{[jk]} = \frac{1}{2} \epsilon^{jkmn} B_i^{[mn]} \tag{2.20}$$

where the tensors $B_{i[mn]}$ can now be directly interpreted in terms of their flavour content as in table 1. Rewriting the invariant (2.19) in terms of the $B_{i[mn]}$ one obtains

$$T_{p.v.} = \frac{1}{2}(b-2c-2d)I_3^- + \frac{1}{2}(a+b-2c)I_4^- \quad (2.21)$$

and

$$T_{p.c.} = (-2a^+ + b^+ + 2c^+ + 2d^+)I_1 - 2a^+I_2 + \frac{1}{2}(-a^+ + b^+ + 2c^+)I_4^+ - 4c^+I_5 \quad (2.22)$$

where we use the following notation for the standard tensor invariants

$$\begin{aligned} I_1 &= \bar{B}^{a[bc]} B_{a[bc']} M_{d'}^d H_{[cd]}^{[c'd']} \\ I_2 &= \bar{B}^{a[bc]} B_{b[c'a]} M_{d'}^d H_{[cd]}^{[c'd']} \\ I_3 &= \bar{B}^{a[bc]} B_{a[b'c']} M_c^d H_{[db]}^{[c'b']} \\ I_4 &= \bar{B}^{b[ca]} B_{a[b'c']} M_c^d H_{[db]}^{[c'b']} \\ \hat{I}_3 &= \bar{B}^{a[bc]} B_{a[b'c']} M_{d'}^{c'} H_{[cb]}^{[db']} \\ \hat{I}_4 &= \bar{B}^{a[bc]} B_{b'[c'a]} M_{d'}^{c'} H_{[cb]}^{[db']} \\ I_5 &= \bar{B}^{a[bc]} B_{\alpha'[b'c']} M_c^{\alpha'} H_{[ab]}^{[a'b']} \end{aligned} \quad (2.23)$$

and $I_i^\pm = I_i \pm \hat{I}_i$.

In order to obtain the final form (2.21) and (2.22) one has to make use of the tracelessness of $H_{[he]}^{[ij]}$ as well as of the Jacobi-type identity for the baryon tensors

$$B_{i[jk]} + B_{j[ki]} + B_{k[ij]} = 0 \quad (2.24)$$

In the case of the p.c. amplitude $T_{p.c.}$ we have made use of the following tensor identity

$$2I_1 = I_3^+ \quad (2.25)$$

in order to reduce the number of tensor invariants in (2.22) to the minimal set of four as is indicated by the analysis (2.16). The amplitudes (2.21) and (2.22) have the advantage that they contain only the necessary minimal number of SU(4) invariants (see eq. (2.16)). Also the tensor contractions avail themselves to a dynamical interpretation in terms of connected quark model diagrams which has numerous advantages as will be discussed in detail in sec. 3.

For the case $1/2^+ \rightarrow 3/2^+ + 0^-$ (and $3/2^+ \rightarrow 1/2^+ + 0^-$) one can directly write down the appropriate representation in terms of the SU(4) tensor invariants and obtains

$$T_{p.c.} = a I_1^{*\mp} + b I_2^{*\mp} \quad (2.26)$$

where

$$\begin{aligned} I_1^{*\pm} &= \bar{B}^{\{abc\}} B_{a[bc']} M_{d'}^d H_{[cd]}^{[c'd']} \pm \bar{B}^{a[bc']} B_{\{abc\}} M_d^{d'} H_{[c'd']}^{[cd]} \\ I_2^{*\pm} &= \bar{B}^{\{abc\}} B_{a[bc']} M_c^d H_{[db]}^{[c'b']} \pm \bar{B}^{a[bc']} B_{\{abc\}} M_d^c H_{[c'b']}^{[db]} \end{aligned} \quad (2.27)$$

Again the tensor invariants are readily interpreted in terms of connected

quark diagrams which greatly facilitates the understanding of these transitions.

Up to this point we have only considered relations among the charm changing transitions. Since the relative strength of the $\Delta C = 1$ and $\Delta C = 0$ parts of \mathcal{H}_{eff} is fixed in principle one can also write down sum rules relating $\Delta C = 1$ and known $\Delta C = 0$ transitions. For example, using $\mathcal{H}_{\text{eff}}^{20''}$ one has the relation

$$t_g^2 \Theta_c (C_0^+ \rightarrow \Delta^{++} K^-)_{\text{p.v.}} = \frac{1}{2} (\Omega^- \rightarrow \Lambda K^-)_{\text{p.v.}} \quad (2.28)$$

where we have neglected possible differences between the renormalized coupling strengths $f_{\Delta C=1}$ and $f_{\Delta C=0}$.

Similar relations can be derived for the transitions $1/2^+ \rightarrow 1/2^+ + 0^-$ where one finds using again $\mathcal{H}_{\text{eff}}^{20''}$ only

$$\begin{aligned} t_g^2 \Theta_c (C_0^+ \rightarrow \Xi^0 K^+)_{\text{p.v.}} &= (6)^{-1/2} (\Sigma^+ \rightarrow n \pi^+)_{\text{p.v.}} \\ t_g^2 \Theta_c (C_0^+ \rightarrow \rho \bar{K}^0)_{\text{p.v.}} &= (3)^{-1/2} (\Sigma^+ \rightarrow \rho \pi^0)_{\text{p.v.}} \\ t_g^2 \Theta_c (T^0 \rightarrow \Xi^0 \bar{K}^0) &= - (\Sigma^- \rightarrow n \pi^-) \\ t_g^2 \Theta_c (C_0^+ \rightarrow \Lambda \pi^+)_{\text{p.c.}} &= -(8)^{-1/2} (\Sigma^+ \rightarrow \rho \pi^0)_{\text{p.c.}} + (6)^{-1/2} (\Xi^- \rightarrow \Lambda \pi^-)_{\text{p.c.}} + 5/2\sqrt{6} (\Lambda \rightarrow \rho \pi^-)_{\text{p.c.}} \\ t_g^2 \Theta_c (C_0^+ \rightarrow \Xi^0 K^+)_{\text{p.c.}} &= (6)^{-1/2} (\Sigma^+ \rightarrow n \pi^+)_{\text{p.c.}} \\ t_g^2 \Theta_c (C_0^+ \rightarrow \rho \bar{K}^0)_{\text{p.c.}} &= -\sqrt{3}/2 (\Sigma^+ \rightarrow \rho \pi^0)_{\text{p.c.}} + 3/2 (\Lambda \rightarrow \rho \pi^-)_{\text{p.c.}} + \sqrt{6} (\Xi^- \rightarrow \Lambda \pi^-)_{\text{p.c.}} \end{aligned} \quad (2.29)$$

It is clear that these relations are expected to be valid only very approximately because of the large mass breaking effects between charmed baryons and ordinary baryons.

Among the $\Delta Y = 1$ hyperon decay amplitudes the $\alpha_{\text{eff.}}^{\Sigma^0}$ leads to the sum rule [21]

$$\sqrt{6} (\Lambda \rightarrow p \pi^-)_{\text{p.v.}} = -\sqrt{2} (\Sigma^+ \rightarrow p \pi^0)_{\text{p.v.}} \quad (2.30)$$

Analogous relations have already been written down in [17]. Concerning the decays involving vector mesons similar sum rules can be written down for the various amplitudes. These are, however, not so useful, since there are no corresponding $\Delta C = 0$ decay amplitudes which could be used for normalization.

III. Quark Model Calculation

A. Decay Amplitudes

In the quark model the effective currentxcurrent Hamiltonian (2.5) gives rise to the 5 types of decay diagrams drawn in fig. 1. We have chosen to label the quark lines for the specific transition $C_6^+ \rightarrow \Lambda \pi^+$ for illustrative purposes. The wavy lines are included in order to indicate how the effective quark currents act.

In terms of quark model wave functions the decay amplitudes corresponding to fig. 1 can be written as

$$\begin{aligned}
 T_{B_1 \rightarrow B_2 + M} = & H_1 \bar{B}_2^{ABC'} B_{1ABC} \bar{M}_D^{D'} (\theta_{C'D'}^{CO} - \frac{1}{3} \theta_{D'C'}^{CO}) \\
 & + H_2 (\bar{B}_2^{AB'D} B_{1ABC} \bar{M}_D^{D'} \theta_{B'D'}^{BC} + \bar{B}_2^{AB'C'} B_{1ABC} \bar{M}_D^B \theta_{B'C'}^{CO}) \\
 & + H_3 \bar{B}_2^{A'B'C'} B_{1ABC} \bar{M}_C^C \theta_{A'B'}^{AB}
 \end{aligned} \tag{3.1}$$

where the first, second and third line of (3.1) correspond to the contributions of diagrams I, II and III in fig. 1 in that order. B_{ABC} and M_A^B are quark model wave functions for the baryons and mesons. Each index A stands for a pair of indices (α, a) , where α and a denote the spin and flavour degrees of freedom. We have already summed over colour degrees of freedom which results in the typical factor $(-1/3)$ in the first line of (3.1). The matrix θ_{AB}^{CD} describes the structure of the effective current current Hamiltonian (2.5), where we have rewritten (2.5) in a more concise notation as

$$\mathcal{H}_{eff.} = : \bar{\Psi}^A \Psi_C \bar{\Psi}^B \Psi_D : \theta_{AB}^{CO} \tag{3.2}$$

H_1 , H_2 and H_3 are wavefunction overlaps corresponding to diagrams I, II and III.

One should note that in the case of transitions between ground state baryons as treated in this paper diagrams II and III obtain contributions only from \mathcal{O}^- (transforming as $20''$ in $SU(4)$), because of the symmetric nature of the ground state baryons [23,24]. Both operators \mathcal{O}^+ and \mathcal{O}^- contribute to diagram I. The contributions of Ia and Ib add up such that the resulting contribution is proportional to $\chi_+ = 1/3(2f_+ + f_-)$ and $\chi_- = 1/3(2f_+ - f_-)$ depending on whether the final state meson is charged or neutral.

For the calculation of the factorizing diagrams Ia and Ib of fig. 1 one does not need to take recourse to the quark model, but these can be directly calculated from the two particle current matrix elements in complete analogy to the evaluation of D- and F-meson decay amplitudes as done in Refs. [15,25]. However, one should already now keep in mind that these factorizing contributions are likely to constitute only a fraction of the total amplitude as will be explicitly shown in sec. 3B. This is different in the mesonic case where the factorizing contributions determine the whole amplitude. The actual calculation of the factorizing contribution corresponding to diagram I is relegated to Appendix A.

The results of calculating diagrams II and III will of course depend on the details of the quark model wave functions which are used as input. In particular, the form of explicit SU(4) symmetry breaking of the resulting amplitudes will depend on how quark and particle masses appear in the wave functions. Undoubtedly these questions will have to be studied in more detail at a later stage. We propose to use the U(2,2) type quark model wave functions of ref. [26] for the evaluation of diagram II and III. The U(2,2) wave functions have recently been applied with good success also to the phenomenology of heavy meson decays [27]. The explicit forms of the wave functions are given by [26] (colour indices are always suppressed and the dependence on internal momenta is not exhibited)

$$\begin{aligned}
 J^P = \frac{1}{2}^+ \quad B_{ABC} &= u_\alpha (\gamma_5 (\not{P}-M)C)_{\beta\gamma} B_{\alpha[bc]} + \text{cycl. } [A,B,C] \\
 J^P = \frac{3}{2}^+ \quad B_{ABC} &= u_\alpha^\mu (\gamma_\mu (\not{P}-M)C)_{\beta\gamma} B_{\alpha[bc]} + \text{cycl. } [A,B,C]
 \end{aligned}
 \tag{3.3}$$

$$\begin{aligned}
 J^{PC} = 0^{-+} \quad M_A^B &= (\gamma_5 (\not{P}-M))_d^B M_a^b \\
 J^{PC} = 1^{--} \quad M_A^B &= (\not{P}-M)_d^B M_a^b
 \end{aligned} \tag{3.4}$$

In (3.3) and (3.4) P and M denote the momentum and mass of the particles and C is the usual charge conjugation matrix. Note that the quark masses do not appear in these wave functions. Symmetry breaking effects enter solely through the use of physical particle masses.

After some straightforward algebraic manipulations involving the evaluation of the amplitude (3.1) with the wave functions (3.3) and (3.4) one arrives at the following amplitudes, where we present our results in terms of invariant amplitudes defined in Appendix B:

Case A $1/2^+ \rightarrow 1/2^+ + 0^-$

$$\begin{aligned}
 A = A^{fac} + \frac{G}{\sqrt{2}} f_c f_- \frac{H_2}{M_1 M_2} & \left(-\frac{3}{8} (M_1 - M_2) Q_+ I_3^+ \right. \\
 & \left. - \frac{3}{8} ((M_1 + M_2) Q_- - 2M_1 M_2 M_3) I_3^- \right)
 \end{aligned} \tag{3.5}$$

$$\begin{aligned}
 B = B^{fac} + \frac{G}{\sqrt{2}} f_c f_- & \left(+\frac{H_2}{M_1 M_2} \frac{1}{8} Q_+ ((M_1 - M_2) I^- + (M_1 + M_2) I^+) \right. \\
 & \left. + \frac{H_3}{M_1 M_2} (+3) M_1 M_2 (M_1 + M_2 + M_3) I_5 \right)
 \end{aligned} \tag{3.6}$$

where $Q_{\pm} = (P_1 \cdot P_2 \pm M_1 M_2)$, $f_c = \cos^2 \Theta_c$ and $I^{\pm} = I_3^{\pm} + 2I_4^{\pm}$. The tensor

invariants I_i^{\pm} have been defined in (2.23). A^{fac} and B^{fac} denote the factorizing contributions which are given in Appendix A. We have factored an explicit mass factor $(M_1 M_2)^{-1}$ from the wave function overlap functions H_2 and H_3 . This assures correct charge normalization when evaluating diagram I with the baryon wave functions (3.3) (one could have equally well factored out the square of the algebraic mean $4(M_1 + M_2)^{-2}$ which is not very different numerically). H_2 and H_3 will be assumed to be channel independent.

One notes that the tensor covariants with the wrong C parity, namely I_3^+ in A and I^- in B, are multiplied with $(M_1 - M_2)$ and thus their contributions vanish in the symmetry limit. There is no contribution of diagram III to the p.v. amplitude. The only contribution to A that survives in the symmetry limit is given by the tensor invariant I_3^- . It is quite intriguing that the same tensor invariant describes the contribution of the ETC-term which arises in the current algebra - soft pion evaluation of the same amplitudes as will be shown in

[†]) In the approach of ref. [28] the contributions of diagrams IIa and III have been neglected without statement of reasons. The result of calculating diagram IIb in [28] agrees with our result which is given by the tensor invariant \hat{I}_3 and $\hat{I}_3 + 2\hat{I}_4$ for A and B, resp.. Note that $\hat{I}_3 = -(\hat{I}_3 + 2\hat{I}_4)/3$ for the decays of C_0^+ and A_0^+ .

Appendix B. ⁺)

Case B $1/2^+ \rightarrow 1/2^+ + 1^-$

In this case there are two p.v. and p.c. amplitudes each which are denoted as A_1, A_2 and B_1, B_2 (see Appendix C). One has

$$A_1 = A_1^{fac} + \frac{G}{\sqrt{2}} f_c f - a_v \frac{H_2}{M_1 M_2} \left((M_1 - M_2) Q_+ I^- / 32 \right. \\ \left. + (M_1 + M_2) Q_- - 2M_1 M_2 M_3 \right) I^+ / 32 \quad (3.7)$$

$$A_2 = \frac{G}{\sqrt{2}} f_c f - a_v \frac{H_2}{M_1 M_2} (M_1 + M_2 + M_3) \left((M_1 - M_2) I^- / 32 + (M_1 + M_2) I^+ / 32 \right) \quad (3.8)$$

$$B_1 = B_1^{fac} - \frac{G}{\sqrt{2}} f_c f - a_v \left(\frac{H_2}{M_1 M_2} Q_+ \left(+ (M_1 - M_2) I^- / 8 + (M_1 + M_2) I^+ / 8 \right) \right. \\ \left. + \frac{H_3}{M_1 M_2} (M_1 + M_2 + M_3) M_1 M_2 (+ 3 I_5) \right) \quad (3.9)$$

⁺) The same equivalence between diagram II and the ETC term holds even for current products with different chiral structure as appears in the calculation of the p.v. NNTT coupling using a product of neutral currents [29]. If this equivalence is not accidental but true in general it would be quite interesting to find out how this equivalence exactly comes about. In this context it is particularly puzzling that the ETC amplitude has one more effective fermion loop and thus there is an additional colour factor of 3 compared to the contribution of diagram II.

$$\begin{aligned}
 B_2 = B_2^{\text{fac}} - \frac{G}{\sqrt{2}} f_c f - a_v \left(-\frac{H_2}{m_1 m_2} (m_1 + m_2) \left((m_1 + m_2) I^+ / 8 + (m_1 - m_2) I^- / 8 \right) \right. \\
 \left. + 3 \frac{H_2}{m_1 m_2} M_3 \left(+ (m_1 + m_2) I_3^+ / 8 + (m_1 - m_2) I_3^- / 8 \right) \right. \\
 \left. - \frac{H_3}{m_1 m_2} 6 m_1 m_2 I_5 \right) \quad (3.10)
 \end{aligned}$$

There is no factorizing contribution to A_2 since we are neglecting as usual the induced pseudoscalar form factor in the axial vector matrix element (see Appendix A). We have allowed for a relative renormalization of the amplitudes involving vector mesons by introducing the factor a_v in (3.7) - (3.10). As in case A the contributions with the wrong C parity vanish in the symmetry limit $m_1 = m_2$. The amplitudes in (3.7) - (3.10) have quite a complex structure and in general all multipole amplitudes contribute to the transition. There is one exception. In the decay $T^0 \rightarrow \Xi^0 \bar{K}^0$ the p.c. transition goes via the transverse multipole M_{1-} since I_3^+ and I_5 are zero for this decay (see (3.9), (3.10) and table 6).

The decays involving $3/2^+$ states have a considerably simpler structure. First, note that the $3/2^+$ wave functions are separately symmetric in flavour and spin indices so that diagrams I Ib and III vanish since $\mathcal{X}_{\text{eff.}}^{20''}$ is antisymmetric in flavour space [30]. Second, diagrams I and I Ib do not interfere since C_0^+ and A_0^+ occur only via diagram I Ib and T^0 only via diagram I as can be seen again by flavour symmetry arguments.

First we consider $1/2^+ \rightarrow 3/2^+ + 0^-$. One has

Case C: $1/2^+ \rightarrow 3/2^+ + 0^-$

$$A = 0$$

(3.11)

$$B = B^{fac} + \frac{G}{\sqrt{2}} f_c f_- \frac{H_2}{M_1 M_2} (M_1 M_2 \frac{3}{2} I_2^{*+}) \quad (3.12)$$

Note that the p.v. amplitude is predicted to be zero [30]. For the factorizing part this results from the assumption that the vector current transition $1/2^+ \rightarrow 3/2^+$ is conserved even for flavour changing transitions. A similar supposition has been made in [31] and is also a result of an explicit quark model calculation [32]. The absence of a p.v. transition from diagram IIa is again analogous to the current algebra + soft pion evaluation which predicts the p.v. amplitude to be proportional to $f_\pi^{-1} \langle 3/2^+ | \mathcal{L}_{p.c.} | 1/2^+ \rangle$ and this is zero in the quark model for the aforementioned reason [30]. The absence of a p.v. amplitude leads to a zero decay asymmetry. This quark model prediction [30] has recently been confirmed in a recent determination of the asymmetry parameter α in the decay $\Omega^- \rightarrow \Lambda K^-$ [33].

As a last case we treat

Case D: $1/2^+ \rightarrow 3/2^+ + 1^-$

$$A_1 = A_1^{fac} + \frac{G}{\sqrt{2}} f_c f_- a_V \frac{H_2}{M_1 M_2} (M_1 Q_+ - M_1 M_2 (M_1 + M_2 + M_3)) (-\frac{3}{2} I_2^{*-}) \quad (3.13)$$

$$A_2 = 0$$

$$A_3 = A_3^{fac} + \frac{G}{\sqrt{2}} f_c f_- a_V \frac{H_2}{M_1 M_2} \frac{3}{2} M_1 I_2^{*-}$$

$$B_1 = B_1^{fac} - \frac{G}{\sqrt{2}} f_c f_- a_V \frac{H_2}{M_1 M_2} M_1 Q_+ \frac{3}{2} I_2^{*+}$$

$$B_2 = B_2^{fac} - \frac{G}{\sqrt{2}} f_c f_- a_V \frac{H_2}{M_1 M_2} M_1 M_2 \frac{3}{2} I_2^{*+} \quad (3.14)$$

$$B_3 = B_3^{fac} - \frac{G}{\sqrt{2}} f_c f_- a_V \frac{H_2}{M_1 M_2} M_1 (-\frac{3}{2} I_2^{*+})$$

By making the appropriate projections one finds that the parity violating amplitude is a mixture of electric and longitudinal multipole amplitudes (no magnetic multipole contribution) and the p.c. transition is a pure M_{1+} transition. Although it may be quite difficult to experimentally disentangle the various multipole transitions in charmed baryon decays it would be extremely interesting to check these predictions of the quark model.

In table 6 and 7 we have listed the results of evaluating the various standard SU(4) invariants for the decays treated in this paper. We have also included the corresponding values for the usual $\Delta C = 0$, $\Delta Y = -1$ hyperon decays. The tables can also be used for the corresponding vector meson decays with the appropriate changes in notation. Concerning the $I = 0$ mesons one has to keep in mind that the physical η , η' , ω and φ mesons are linear combinations of the η_8 and η_1 states appearing in the tables. The relevant combinations are given in the caption of table 6. One can check that the various sum rules and the identity (2.25) written down in sec. 2 are satisfied by the entries of table 6.

As a last remark we would like to point out that the nonfactorizing quark model amplitudes in (3.5) - (3.14) possess remarkable properties in the limit of M_1 becoming large. This limit may not yet be relevant for charmed baryon decays but may be profitably studied in the decays of the next heavy baryons with bottom quantum numbers. In the large M_1 limit only contributions from diagram IIa survive in which the heavy quark first decays weakly and then emits a meson. All helicity amplitudes are of the order $(M_1)^3$ which is a result of subtle cancellations among the invariant amplitudes contributing to the helicity amplitudes. For example, in the case $1/2^+ \rightarrow 3/2^+ + 1^-$ these cancellations occur at the leading and next to leading order level.

The resulting widths are of order $\Gamma \approx M_1^5$. If one would have factored the algebraic mean $4(M_1 + M_2)^{-2}$ from the amplitudes one would have obtained $\Gamma \approx M_1^3$ similar to the large M_1 behaviour of heavy meson decays studied in [27, 2nd reference]. Whereas the factorizing contributions in (3.5) - (3.14) have a simple helicity structure in the large M_1 limit reflecting the basic (V-A) heavy quark decay this is no longer true for diagram IIa. Thus heavy baryon nonleptonic decays are not so well suited to study the basic heavy quark decay property as are e.g. the heavy meson decays which obtain contributions only from factorizing contributions. [27, 2nd reference].

III B Numerical Results

The quark model amplitudes calculated in sec. 3A contain a number of parameters (i.e. f_+ , f_- , H_2 and H_3) which have to be estimated in order to be able to make any quantitative predictions about decay widths, branching ratios, asymmetry parameters etc.. Since estimates of these parameters are at present afflicted with theoretical uncertainties, it is clear that those predictions of our quark model calculation must be considered most reliable which are independent of the particular values of the above parameters. A glance at

table 6 shows that the quark model amplitudes for the cases $1/2^+ \rightarrow 1/2^+ + 0^-(1^-)$ (3.5), (3.6) and (3.7-3.10) are sufficiently complex that there are no parameter independent predictions which go beyond the I, U and V sum rules given in sec. 2. However, in the cases $1/2^+ \rightarrow 3/2^+ + 0^-(1^-)$ the quark model amplitudes are sufficiently simple so that the resulting structure is parameter independent to a considerable degree. Among these predictions are the zero asymmetry in the decays $1/2^+ \rightarrow 3/2^+ + 0^-$, the M_{1+} structure of the p.c. amplitudes for $1/2^+ \rightarrow 3/2^+ + 1^-$, and the vanishing of the decay modes $A^+ \rightarrow \Sigma^{*+} \bar{K}^0 (\bar{K}^{0*})$ and $A^+ \rightarrow \Xi^{*0} \pi^+ (\mathcal{S}^+)$.

Further results are obtained by fixing the parameter values. For the short distance enhancement factor $f_{-}^{\Delta C=1}$ which may be calculated by considering the renormalization of the weak vertex due to hard gluon exchange [9] we take a value which lies in the middle of the range of estimates proposed in refs. [13], [15] and [16] and thus

$$f_{-}^{\Delta C=1} = 1.9 \quad f_{+}^{\Delta C=1} = (f_{-}^{\Delta C=1})^{-1/2} = 0.73 \quad (3.15)$$

which leads to

$$\chi_{+}^{\Delta C=1} = 1.12 \quad \chi_{-}^{\Delta C=1} = -0.15 \quad (3.16)$$

For the values of the quark model wave function overlap parameters H_2 and H_3 we use the best fit values of ref. [30] which were obtained from a fit to the ordinary $\Delta C = 0$ nonleptonic hyperon decays. Thus we

take ⁺)

$$f_{-}^{\Delta C=0} \cdot H_2 = 0.75 \text{ GeV} \quad (3.17a)$$

$$f_{-}^{\Delta C=0} \cdot H_3 = -0.62 \text{ GeV} \quad (3.17b)$$

There exist two independent checks on the value of H_2 in (3.17a). Firstly, the hyperon beam experiment at the CERN SPS produced a data sample of $> 1000 \Omega^-$ which resulted in a new Ω^- partial width determination of [33]

$$\Gamma_{\Omega^- \rightarrow \Lambda K^-} \sim 0.8 \times 10^{10} \text{ sec}^{-1} \quad (3.18)$$

The same experiment showed that the asymmetry in this decay is consistent with zero, as predicted in our quark model. Since there are no factorizing contributions to $\Omega^- \rightarrow \Lambda K^-$ the quark model rate is proportional to $|H_2|^2$ (see eq. (3.12)). Using the numerical value (3.17a) we calculate $\Gamma_{\Omega^- \rightarrow \Lambda K^-} = 0.64 \times 10^{10} \text{ sec}^{-1}$. The agreement is satisfactory. A second indirect confirmation of the value of (3.17a) comes from a recent calculation of the matrix element $\langle B' | \mathcal{H}_{p.c.} | B \rangle$ using harmonic oscillator wavefunctions for the baryons [34]. The above matrix element determines the properties of the non-leptonic hyperon decays (see next section) and its calculated value is in agreement with the best fit value found in ref. [35] if the currently accepted values of $f_{-}^{\Delta C=0}$ are properly included. Since

⁺) Our normalization of H_2 and H_3 differs from that of ref. [30].

latter approach was found to be equivalent to the quark model calculation (see sec. 4 and [30]) the calculation of ref. [34] gives further support to the estimate (3.17a). There is no independent check on the value of H_3 in (3.17b). The value (3.17b) was determined in ref. [30] by a common fit to the p-wave hyperon decays.

Recently there has been an interesting suggestion by Shifman et al. [36] who argue that there exist an additional SU(4) 15 contribution to the $\Delta C = 0, \Delta Y = -1$ nonleptonic hyperon decays that arise from soft gluon effects. They evaluated the gluon exchange diagram fig. 2 and found that its contribution to the operator product expansion due to imperfect GIM cancellation from soft gluon contributions may be larger than had been previously assumed. The main effect of this new term is to considerably enhance and change the structure of the factorizing contributions corresponding to diagram I. One finds that this would imply a corresponding reduction of the contributions of diagrams II and III if the same hyperon decay data were fitted. This in turn would result in a lowering of the fit values of H_2 and H_3 . Since this new term is not effective in the $\Delta C = 1$ case, this would directly result in a reduction of the charm changing decay rates compared to an evaluation using (3.17). We believe that the authors of ref. [36] have considerably overestimated the contribution of diagram fig. 2. Apart from theoretical arguments that can be raised against the choice of certain parameters used in [36] that enhance the contribution of fig. 2 one can directly confront the resulting prediction for the rate of e.g. $\Omega^- \rightarrow \Xi^0 \pi^-$ with the recent experimental value

$$\Gamma_{\Omega^- \rightarrow \Xi^0 \pi^-} \sim 0.3 \times 10^{10} \text{ sec}^{-1} \quad (3.19)$$

from the CERN hyperon beam experiment [33].

The decays $\Omega^- \rightarrow \Xi^0 \pi^0$ provide a clean test of quark models since only diagram I contributes. Using the model parameters of ref. [36] one calculates $\sim 2 \times 10^{10} \text{ sec}^{-1}$ for (3.19) whereas one finds $\sim 0.11 \times 10^{10} \text{ sec}^{-1}$ if the soft gluon corrections are omitted. This shows that there is some room for such a new term, however, not at the strength proposed in [36]. We have checked that the inclusion of such a small additional contribution improves the overall fit to the $\Delta C = 0 \ 1/2^+ \rightarrow 1/2^+ + 0^-$ nonleptonic hyperon decays in [30], without, however, affecting the fit values H_2 and H_3 (3.17) appreciably.

In the realm of charmed baryon decays the importance of the contributions of diagrams II and III may be indirectly appreciated by calculating decay rates using diagram I alone. From tables 6 and 7 it is clear that only a very small number of possible charmed baryon decay channels are fed from diagram I. From these one obtains the rates

$$\begin{aligned}
 \Gamma_{C_0^+} &= 1.27 \times 10^{12} \text{ sec}^{-1} \\
 \Gamma_{A^+} &= 1.77 \times 10^{12} \text{ sec}^{-1} \\
 \Gamma_{A^0} &= 1.79 \times 10^{12} \text{ sec}^{-1} \\
 \Gamma_{T^0} &= 8.04 \times 10^{12} \text{ sec}^{-1}
 \end{aligned}
 \tag{3.20}$$

This has to be compared with the corresponding semileptonic rates as calculated by Buras [31] (into e or μ)

$$\begin{aligned}
 \Gamma_{\rho^+}^{s.p.} &= 0.6 \times 10^{12} \text{ sec}^{-1} \\
 \Gamma_{A^+}^{s.p.} &= 1.45 \times 10^{12} \text{ sec}^{-1} \\
 \Gamma_{A^0}^{s.p.} &= 1.45 \times 10^{12} \text{ sec}^{-1} \\
 \Gamma_{T^0}^{s.p.} &= 1.44 \times 10^{12} \text{ sec}^{-1}
 \end{aligned}
 \tag{3.21}$$

If the contributions from diagrams I were really dominant, one would obtain very large semileptonic branching ratios which seems unreasonable from what is known for the corresponding charmed meson decays.

Returning now to (3.17) we note that the fit to the hyperon decay data can only determine the product of $f_{-}^{\Delta C=0}$ with the wave function overlap parameters H_2 and H_3 . One expects $f_{-}^{\Delta C=0} > f_{-}^{\Delta C=1}$ on general grounds since the average effective mass of the quarks and thus the subtraction point for evaluating the hard gluon corrections is lower for $\Delta C = 0$ decays [13,16]. For the ratio of $f_{-}^{\Delta C=0}$ and $f_{-}^{\Delta C=1}$ we use the same value as in our previous calculation [6]

$$f_{-}^{\Delta C=1} / f_{-}^{\Delta C=0} = 0.54
 \tag{3.22}$$

which is at the lower end of the range of values calculated in [16]. Uncertainties in the theoretical determination of the ratio (3.22) would change our rate estimates accordingly.

Concerning the vector meson weight factor Q_V in (3.7-3.10), (3.13) and (3.14)

we note that $a_V = 1$ in a pure U(2,2) approach. Since, however, the same model predicts $f_{\rho^+} / f_{\pi^+} (= f_{\kappa}) = 1/m_{\rho}$ (see eq. (3.4)) compared to the experimental value $\sim 1.46/m_{\rho}$ we have decided to multiply the vector meson amplitudes by the factor 1.46.

All the parameters appearing in the quark model amplitudes are now fixed and one can proceed in the evaluation of the numerical predictions of our model. We reiterate at this point that due to the theoretical uncertainties involved in estimating some of the parameters the numerical results should be treated with a certain amount of caution. Nevertheless we felt that it would be useful to present our results also in a definite numerical form in order to provide a guiding pattern for the analysis of charmed baryon decay data expected in the near future.

In table 8 we have listed partial decay rates for the decays $1/2^+ \rightarrow 1/2^+ + 0^-$ as well as values for the asymmetry parameter defined by

$$\alpha = - \frac{2k \operatorname{Re} AB^*}{|A|^2 + k^2 |B|^2} \quad (3.23)$$

The asymmetries are in general close to their maximal (minimal) possible value +1 (-1) indicating that p.v. and p.c. amplitudes contribute equally to the decay width. For $C_0^+ \rightarrow \Xi^0 K^+$ and $A^0 \rightarrow \Sigma^+ K^-$ the asymmetry is zero caused

[†]) Our rate values sometimes differ from those given in [6]. This is due to using a slightly different $f_{\Delta C=1}$ and the introduction of $\eta-\eta'$ mixing. Note that the $\sim -10^\circ$ mixing angle used here has an appreciable effect on the calculated rates in some cases.

by the absence of a p.v. contribution. This follows directly from the vanishing of the invariant I_3 for these decays (see table 6).

In table 8 we have also listed the corresponding SU(4) predictions. We have used SU(4) for the dimensionless amplitudes A and B, $20''$ -dominance for α_{eff} and hyperon decay data in the manner of [17] supplemented by the T^0 sum rule in (2.29). The resulting amplitudes were scaled by the ratio of enhancement factors (3.22).

In general there are large discrepancies between the SU(4) and quark model results for both rates and asymmetries. Note in particular the factor 20 difference in the predicted rates for $T^0 \rightarrow \Xi^0 \bar{K}^0$ and the difference in the predicted asymmetry α for $C_0^+ \rightarrow \Lambda \pi^+$. For the latter SU(4) predicts $\alpha = 0$ due to the vanishing of the p.v. contribution (see (2.10) and also [18]). The discrepancies between the results of the two models can directly be traced to the explicit mass breaking factors present in our quark model approach. Measurements of branching ratios and asymmetry parameters are necessary to resolve the question of the importance of symmetry breaking effects in the decay of charmed baryons. A discussion of the current algebra plus soft pion results given in table 8 will be presented in sec. 4.

In table 9 we have given the results of our quark model calculation for the decays $1/2^+ \rightarrow 3/2^+ + 0^-$. One notes the predicted vanishing of $A^+ \rightarrow \Sigma^{*+} \bar{K}^0$ and $A^+ \rightarrow \Xi^{*0} \pi^+$. The same result was obtained in sec. 2 using SU(4) and $20''$ dominance for α_{eff} . The quark model result is more powerful in that it predicts a vanishing rate for a general mixture of $\alpha_{\text{eff}}^{20''}$ and α_{eff}^{84} . Note also the small value predicted for the rate $T^0 \rightarrow \Xi^{*0} \bar{K}^0$ which is due

to the fact that this decay proceeds via diagram I and is proportional to the small $\chi_{-}^{\Delta C=1}$ (3.16). The small rate for $A^0 \rightarrow \Xi^{*0} \bar{K}^0$ is a consequence of $\eta_1 - \eta_8$ mixing which in this case effects an almost complete cancellation of the relevant η_1 and η_8 contributions.

We have also included in table 9 SU(4) predictions using SU(4) symmetry for the dimensionless amplitude $B(M_1 + M_2)$, 20^+ dominance for χ_{eff} and as input the $\Omega^- \rightarrow \Lambda K^-$ rate (3.18). We also assume that the decay is entirely parity conserving which is consistent with the data (see discussion following (3.18)). From drawing decay diagrams or explicitly from table 7 one notices that the C_0^+ and A_0^+ decays are directly related to $\Omega^- \rightarrow \Lambda K^-$, whereas $T^0 \rightarrow \Omega^- \pi^+$ and $T^0 \rightarrow \Xi^{*0} \bar{K}^0$ are related to $\Omega^- \rightarrow \Xi^0 \pi^0$. We have refrained from giving SU(4) predictions for $T^0 \rightarrow \Omega^- \pi^+$ and $T^0 \rightarrow \Xi^{*0} \bar{K}^0$ for several reasons. First there may be a SU(4) 15 contribution to $\Omega^- \rightarrow \Xi^0 \pi^0$ as discussed above (see also [37]) which means that it may be too naive to use the experimental $\Omega^- \rightarrow \Xi^0 \pi^0$ rates as input in the SU(4) calculation. Secondly such a comparison depends on the values of the ratios $\chi_{\pm}^{\Delta C=1} / \chi_{\pm}^{\Delta C=0}$ which are quite sensitive to input assumptions. Otherwise the predicted SU(4) rates are not very different from the quark model predictions which reflects the simple structure of these transitions.

In table 10 and 11 we have given rate predictions for the cases $1/2^+ \rightarrow 1/2^+ + 1^-$ and $1/2^+ \rightarrow 3/2^+ + 1^-$. Future measurements will be able to test these predictions.

Summing up all the partial rates in tables 8-11 we arrive at the following total rates for the quasi two body decays.

$$\begin{aligned}
 \Gamma_{\phi^+} &= 12.9 \times 10^{12} \text{ sec}^{-1} \\
 \Gamma_{A^+} &= 3.9 \times 10^{12} \text{ sec}^{-1} \\
 \Gamma_{A^0} &= 18.7 \times 10^{12} \text{ sec}^{-1} \\
 \Gamma_{T^0} &= 18.4 \times 10^{12} \text{ sec}^{-1}
 \end{aligned}
 \tag{3.24}$$

As argued before, this rate should already be quite close to the total hadronic rate. The above rates are larger than the free quark model estimate of Ellis et al., who quote $\sim (1.5 \text{ to } 2) \times 10^{12} \text{ sec}^{-1}$ for $m_c = 1.5 \text{ GeV}$ and $\sim (6 \text{ to } 8) \times 10^{12} \text{ sec}^{-1}$ for $m_c = 2 \text{ GeV}$ [13]. Their rate estimates is closer to the numbers given in (3.24) for the factorizing contributions which shows that the more complicated quark transitions occurring in diagrams II and III may not be adequately estimated by calculating the decay of a free quark. In the same vain the fact that $\Gamma_{A^+} \ll \Gamma_{A^0}$ compared to the free quark model prediction $\Gamma_{A^+} = \Gamma_{A^0}$ reflects the lack of possible decay channels for A^+ compared to A^0 which cannot be accounted for in the free quark model.

The fact that $\Gamma_{\phi^+} \sim \Gamma_{A^0}$ reflects the fact that the dominant piece of the transition comes from diagrams II and III and thus from the $20''$ piece in the weak Hamiltonian. Equality of Γ_{ϕ^+} and Γ_{A^0} is expected for $20''$ dominance in the symmetry limit (see (2.7) and [17]), as well as for rates into specific spin configurations. Our results are close to these predictions and the deviations from equality are mostly due to mass breaking effects.

By comparison with the semileptonic widths of Buras [31] (see eq. (3.21)) we arrive at semileptonic branching ratios (e or μ) of 4 %, 37 %, 7 % and 8 % for C_0^+ , A^+ , A^0 and T^0 . As we shall argue in the following one mostly expects to see decaying C_0^+ 's in the energy region above charm baryon threshold. If the above semileptonic branching ratio of 4 % for C_0^+ reflects the total semileptonic branching ratio this would mean that the semileptonic branching ratio of charmed baryons can be expected to be approximately half of that of charmed mesons.

From the partial widths in tables 8-11 one can calculate inclusive p , Λ and Σ decay rates by considering the various possible decay chains with their known branching ratios [38]. One finds (in units of 10^{12} sec^{-1})

$$\Gamma_{C_0^+ \rightarrow p+X} = 5.7 + 2.0 + 1.8; \Gamma_{C_0^+ \rightarrow \Lambda+X} = 3.2; \Gamma_{C_0^+ \rightarrow \Sigma^\pm+X} = 3.4 \quad (3.25)$$

where the inclusive proton rate is the full inclusive rate. The second and third term in the sum $\Gamma_{C_0^+ \rightarrow p+X}$ represents contributions from Λ and Σ decays which have to be subtracted if these subsamples have been removed from the data. The inclusive rates in (3.25) suggest that the yield of Λ 's and Σ 's from C_0 -decays is approximately 33 % of the (full) yield of protons. This is in qualitative agreement with some recent experiments in e^+e^- annihilation [1], where a signature of charmed baryon production was observed in inclusive baryon production when the e^+e^- energy was raised above charmed baryon threshold. The additional yield of baryons was observed to be strongest in the \bar{p} -channel and occurred at a considerably reduced rate of $\sim 15\%$ in the $\bar{\Lambda}$ -channel [1]. Our calculated inclusive rates (3.25) show that the C_0^+ preferentially decays into p's compared to Λ 's, however, the effect is

not as big as indicated by the data ⁺⁾ .

If the experimentally observed large suppression of excess Λ 's (or $\bar{\Lambda}$'s) persist in future data , one may have to look for sources other than C_0^+ for excess baryons. One possibility would be that one is also observing weak decays of the C_1^0 and C_1^{++} members of the C_1 isotriplet. This could be the case if the mass values of the C_1 isotriplet turn out to be lower than the QCD estimate of [11] which could mean that C_1^0 and C_1^{++} have to decay weakly

⁺⁾ A heuristic explanation of the predominance of p's over Λ 's may be obtained from the following argument. The flavour wave function of the proton contains fewer terms than that of the Λ . This is connected to the fact that the proton lies on the edge of the SU(3) weight diagram whereas Λ lies in its centre. Therefore each wave function component in p carries a higher weight than those of the Λ since both wavefunctions are normalized to the same value. Since the weak transition \mathcal{H}_{eff} connects only to selected wave function components in p and Λ the net result is that transitions to protons are favoured. This enhancement mechanism is explicit in the entries of table 6 where we have factored out the normalization factor of the quark states in each separate flavour channel. The remaining coefficients are all of the same magnitude so that the strength of a transition is on the average determined by the inverse of the normalization factor which is big for particles lying in the center of weight diagrams and small for particles on the edges. A striking example of this enhancement mechanism is provided by the decay $T^0 \rightarrow \Xi^0 \bar{K}^0$ where all three particles lie on the edges of the respective SU(4) weight diagrams and where the normalization factor is therefore 1.

because of phase space reasons.

There also exist some inclusive $\bar{\Sigma}$ -data in e^+e^- -annihilation which shows that the yield of $\bar{\Sigma}$'s also increases after charmed baryon threshold [2]. The increase in the inclusive yield was estimated at $\Delta R_{\bar{\Sigma}} \sim .12 \pm .05$. It is not clear how relevant this data is to our analysis since the data taken above charmed baryon threshold are at 6 - 7 GeV. The above $\Delta R_{\bar{\Sigma}}$ is $\sim 75\%$ of the $\Delta R_{\bar{p}}$ measured in [1]. A reduction of the $\bar{\Sigma}$ -rate relative to \bar{p} is also indicated in our calculated rates (3.25) which give a relative rate of 36% and is somewhat smaller than the above number. One important observation concerns the fact that our results predict that 99% of the inclusive Σ rate from C_0 -decays consist of Σ^+ 's (and 1% of Σ^- 's) which should be checked in future charmed baryon production experiments.

For the decays of the other charmed baryons $A^{+,0}$ (T^0) we expect the inclusive rates to be weighted more towards the Λ and Σ channels since the decaying charmed baryons carry one (two) more units of strangeness so that the baryon decay products should carry on the average one (two) more units of strangeness. This is borne out by explicit calculation. We find (in units of 10^{12} sec^{-1})

$$\Gamma_{A^+ \rightarrow p+X} = 0 + 1.1 + 1.1 ; \Gamma_{A^+ \rightarrow \Lambda+X} = 1.7 ; \Gamma_{A^+ \rightarrow \Sigma^\pm+X} = 2.2 \quad (3.25)$$

$$\Gamma_{A^0 \rightarrow p+X} = 0 + 9.2 + 2.3 ; \Gamma_{A^0 \rightarrow \Lambda+X} = 14.4 ; \Gamma_{A^0 \rightarrow \Sigma^\pm+X} = 4.4 \quad (3.26)$$

and T^0 decays into $\Lambda + X$ 100% of the time. Again the inclusive Σ^\pm rates are made out of inclusive Σ^+ 's 99% of the time.

If the $A^{+,0}$ and T were copiously produced in e^+e^- annihilation above their respective thresholds, their decays would primarily feed into the Λ -inclusive channels. This makes the lack of observation of additional Λ 's in the Spear experiment even more puzzling since most of the data is taken in an energy region where pair production of A's and T's could occur. We believe, however, that pair production of A's and T's is considerably suppressed relative to the production of the lower lying charmed baryons, due to form factor effects. In fact, making a simple ansatz for the electromagnetic form factors of charmed baryons based on a dipole Ψ, Ψ' vector dominance picture one arrives at the following relative production rates

$$C_0\bar{C}_0 : A\bar{A} : T^0\bar{T}^0 \sim 1 : 0.2 : 0.05 \quad (3.27)$$

This shows that the decay characteristics of C_0^+ -decays should in fact determine the additional baryon yield after charmed baryon threshold to a high degree.

As a last point we discuss the average multiplicity into charged and into all particles for C_0^+ -decays. Using known branching ratios for the particles in the decay chains we calculate ⁺⁾

$$\langle n_{ch} \rangle = 2.7 \quad (3.28)$$

and

$$\langle n_{all} \rangle = 3.9 \quad (3.29)$$

⁺⁾ We count K_S^0 as two particles and take K_L^0 to go undetected

This means that the C_0^+ decays on the average into several particles and should be looked for in multibody final states. Also one expects jet-like configurations since the particles originate mostly from resonances. The average multiplicity $\langle n_{\text{all}} \rangle$ is approximately the same as given in the statistical model [7,10] so that measurements of this quantity are not useful to discriminate among these two models. The corresponding numbers for A_0^+ and T_0^+ decays are quite similar and are not given here.

IV. Current Algebra Results

Since the current algebra plus soft pion technique has led to a plausible description of the nonleptonic hyperon decay data in $1/2^+ \rightarrow 1/2^+ + 0^-$ it is quite natural to try and extend this method to study the corresponding charmed baryon decays. We shall do this extension in the most straightforward manner in the spirit of SU(4), being, however, aware that the different kinematical range involved in latter decays may require additional considerations. Least one worry that the soft pion, kaon and eta extrapolation necessary in latter application are problematic we refer to the interpretation of the current algebra plus soft pion method in terms of quark diagrams which ameliorates some of these misgivings [30].

The current algebra plus soft pion method for the description of nonleptonic hyperon decays have been discussed in detail in [35,39] and we therefore ^{only} need to give a brief recapitulation here. The transition amplitude $B_i \rightarrow B_j + P_k$ is written as

$$\begin{aligned}
 T_{ijk} &= \langle P_k B_j | \mathcal{H}_w(0) | B_i \rangle \\
 &= \bar{u} (A_{ijk} + B_{ijk} i\gamma_5) u
 \end{aligned}
 \tag{4.1}$$

The LSZ reduction technique allows one to reduce the pseudoscalar meson in the final state. The off-shell meson field is then related to the corresponding axial vector current using PCAC. Finally, one exploits the current algebra commutation relation between the weak Hamiltonian and the axial vector and vector currents. Explicit pole contributions due to near by ground state mesons and baryons are separated off and retained before the soft meson limit is taken. The result of these manipulations are given by the following expressions:

$$A_{ijk} = A_{ijk}^{\text{fac}} - \frac{1}{f_P} \langle B_j | [Q_k(0), \mathcal{H}_{p.c.}(0)] | B_i \rangle
 \tag{4.2}$$

$$B_{ijk} = B_{ijk}^{\text{fac}} + \sum_m \frac{g_{jmk} S_{im}}{M_m - M_i} + \sum_n \frac{g_{ink} S_{jn}}{M_j - M_n}
 \tag{4.3}$$

The 2nd term in (4.2) is usually referred to as the equal time commutator term A_{ijk}^{ETC} . In (4.2) f_P denotes the reduced pseudoscalar meson decay constant. $Q_k(0)$ is the SU(4) charge with the quantum numbers of the meson P_k and operates on the baryon states to its left and right as a SU(4) generator. Thus the matrix element in (4.2) is reduced to a sum of terms of the form

$$\langle B_2 | \mathcal{H}_{p.c.} | B_1 \rangle = \bar{u} S_{12} u \quad (4.4)$$

where both B_1 and B_2 are members of the $20'$ multiplet. The same spurion amplitude S_{ij} appears also in the pole contributions to the p.c. amplitude B_{ijk} in (4.3) since the sum over pole contributions in B_{ijk} is usually assumed to be well approximated by the ground state baryons. The strong coupling constant g_{jmk} appearing in (4.3) denotes the strong coupling ($B_j \bar{B}_m P_k$). A_{ijk}^{fac} and B_{ijk}^{fac} denote the factorizing contributions as given e.g. in Appendix A. The relative scale and phase between the p.v. and p.c. amplitude is set by the generalized Goldberger Treiman relation which gives

$$f_{P_k} = \frac{(g_A)_{ijk} (M_i + M_j)}{g_{ijk} \sqrt{2}} \quad (4.5)$$

Before evaluating (4.2) numerically we wish to make some comments on how the SU(3) application of (4.2) to the ordinary nonleptonic hyperon decays appears in the light of the discovery of SU(4). It is well known that the symmetric coloured quark model predicts that only the octet component of $\mathcal{H}_{p.c.}$ contributes to the matrix element (4.2) at the level of SU(3) [23,24]. There are then two SU(3) tensor invariants describing (4.4) corresponding to a general F and D structure. One possible coupling is given by

$$I = \bar{B}^{m[ke]} B_{m[ig]} H_{[ke]}^{[ig]} \quad (4.6)$$

which can be seen to correspond to a F/D ratio of -1. The other SU(3) tensor invariants involve contractions within $H_{\{kl\}}^{[ij]}$. The rationale for using only the tensor invariant (4.6) and thereby a F/D = -1 for the matrix element (4.4) in the old quark model calculations was based on rather imprecise notions of connectedness of quark line diagrams [30,35]. The rationale for using only (4.6) is now of course provided by the GIM mechanism which tells us that contractions within $H_{\{kl\}}^{[ij]}$ cancel (or almost cancel [36]). This is also the reason that some SU(4) results for the SU(3) sector of hyperon decays were already anticipated in the pre-SU(4) calculations, as e.g. the ratio D/F = -1 which leads to the sum rule (2.30) and the vanishing of the matrix elements $\langle B_{10} | \mathcal{H}_{p.c.} | B_8 \rangle$ and $\langle B_{10} | \mathcal{H}_{p.c.} | B_{10} \rangle$ [23].

The factorizing contributions in (4.2) correspond to the K- and K* contributions of [35,40] which were estimated from a pole model description of non-leptonic K-decays. The size of the K and K* contributions used in [35,40] are in general larger than what one calculates directly from the factorization prescription. This is of course again a reflection of the fact that the non-leptonic enhancement calculated from hard gluon exchange is not sufficient to explain the $\Delta C = 0$ transition amplitudes.

For the charm changing transition one believes that the calculation of the renormalization effects due to hard gluon exchange is more reliable since the mass scale is higher for the charm changing processes [13,16]. Thus one anticipates that the factorizing parts in (4.2) are well accounted for by the estimates in Appendix A. In order to fix our notation we give the results of evaluating the amplitudes (4.2) for the two transitions $C_0^+ \rightarrow \Lambda \pi^+$ and $A^0 \rightarrow \Lambda \bar{K}^0$.

1. $C_0^+ \rightarrow \Lambda \pi^+$

$$A = A^{fac}$$

$$B = B^{fac} + 4(6)^{-1/2} F' g (C_0^+ + \Lambda) \left(-\frac{f}{(\Sigma^+ - C_0^+)(\Sigma^+ + \Lambda)} + \frac{f}{(\Lambda - C_1^0)(C_1^0 + C_0^+)} \right) \quad (4.7)$$

2. $A^0 \rightarrow \Lambda \bar{K}^0$

$$A = A^{fac} + (6)^{1/2} F' f_K^{-1}$$

$$B = B^{fac} + 2(6)^{1/2} F' g (A^0 + \Lambda) \left(\frac{(3f-d)^3}{(\Sigma^+ - C_0^+)(\Sigma^+ + \Xi^0)} - \frac{f}{(\Sigma^0 - C_1^0)(C_1^0 + A^0)} \right) \quad (4.8)$$

$$2 F' = \frac{G}{\sqrt{2}} \cos^2 \theta_c \frac{R}{8} \left(f_{-}^{\Delta C=1} / f_{-}^{\Delta C=0} \right)$$

In (4.7) and (4.8) we have used particle symbols for the masses of the particles. m_N is the mass of the nucleon, g the strong coupling $g = 13.5$, $(d+f) = \sqrt{2}$, $d/f = 1.73$ in agreement with the factorizing part and $F' = 12.3 \times 10^{-8}$ GeV as follows from the fit in [35]. We have used SU(4) for the axial vector coupling which means that the strong coupling is broken according to the generalized Goldberger Treiman relation (4.5). The amplitudes for the other processes follow from (4.7) or (4.8) by simply applying SU(4) to the relevant matrix elements.

Because of the particular nature of the symmetry breaking of g_{ijk} which favours coupling to heavy baryons the second term in the p.c. amplitude dominates. These are the contributions where the charmed baryon first emits a meson and then undergoes the $\Delta C = 1$ transition. This is different from the quark model approach where we found that the dominant contribution in the case of large M_1 masses occurs in the configuration diagram II_a where the charmed quark first decays

into a noncharmed quark and then emits the meson. The nonfactorizing contributions in (4.2) are of lower order in M_1 than the factorizing parts which is again different from the quark model, where both parts are of similar order.

The numerical results appear in the last two columns of table 8. When comparing with the quark model results there does not seem to be an apparent trend of deviations, whereas differences between the two set of results are pronounced for some single channels. Future experimental results have to decide which of the two sets of predictions are closer to reality.

5. Summary and Conclusions

We have argued that charmed baryons decay predominantly into two body and quasi two body final states belonging to the ground state baryons and mesons. We have presented the results of a quark model calculation of these decays starting from an effective weak Hamiltonian that incorporates hard gluon exchange effects. We give detailed predictions for branching rates and asymmetry parameters. We found that decays into states at the edges of flavour symmetry weight diagrams are favoured which may explain why more protons than Λ 's are seen from charmed baryon decays.

We have stressed that some of our quark model predictions are quite model independent, as e.g. the predicted multipole structure or vanishing of certain decay modes. Other predictions depend on parameter choices and on the way mass breaking effects are incorporated in the quark model wave functions. We found that SU(4) sum rules that are based on the SU(4) charge conjugation

property of the decay amplitudes are badly broken in the quark model whereas sum rules that are based only on the I, U and V spin properties of the interaction are approximately satisfied. Due to the dominance of a certain class of quark model diagrams the transitions are also well approximated by 20° dominance. We have also given SU(4) and current algebra plus soft pion prediction for certain spin channels. There are large differences between the predictions of the three models which can be tested in future experiments. Our total life time estimates are 5-10 times smaller than the free quark model estimates. Reasons for this discrepancy are pointed out.

Summarily speaking, the phenomenology of charmed baryon decays provide us with a rich testing ground for our ideas on how on the one hand quarks weakly interact with each other at short distances and how on the other hand the fundamental quark interaction is imprinted on the quarks in the final states which are bound by long distance forces. We have tried to raise some of these issues by doing some explicit calculations in this paper and hope to have provided some stimulus for further theoretical and experimental work on these problems.

Acknowledgement

We would like to thank G. Flügge and P. Le Comte for discussions on experimental questions. A helpful correspondence with J. Timmermans on Ω^- decays is acknowledged.

Appendix A - Factorizing Contributions

The current matrix element of two baryons belonging to the $20'$ has in general two $SU(4)$ reduced matrix elements which can be specified in terms of the measured form factors of current transitions involving known baryons as has been discussed by Buras [31]. In the charm changing case one finds, by following the quark lines in diagram I, that the only possible contributions come from transitions that involve a charged π^+ (or ρ^+) or a neutral \bar{K}^0 (or \bar{K}^{*0}) in the final state. The results of calculating the factorizing contribution can be conveniently expressed by the two tensor invariants I_1 and I_2 defined in (2.23) and calculated for individual processes in Table 6. For $1/2^+ \rightarrow 1/2^+ + 0^-$ one has

$$\begin{aligned}
 A^{fac} &= \frac{G}{\sqrt{2}} \chi_{\pm} f_c f_P (M_1 - M_2) \left(\frac{3}{2} (I_1 + I_2) H_1^{(3^*)} + \frac{1}{2} (I_1 - I_2) H_1^{(6^*)} \right) \\
 B^{fac} &= -\frac{G}{\sqrt{2}} \chi_{\pm} f_c f_P (M_1 + M_2) \left(\frac{3}{2} (I_1 + I_2) H_3^{(3^*)} + \frac{1}{2} (I_1 - I_2) H_3^{(6^*)} \right)
 \end{aligned} \tag{A 1}$$

and for $1/2^+ \rightarrow 1/2^+ + 1^-$

$$\begin{aligned}
 A_1 &= \frac{G}{\sqrt{2}} \chi_{\pm} f_c m_V^2 f_V \left(\frac{3}{2} (I_1 + I_2) H_3^{(3^*)} + \frac{1}{2} (I_1 - I_2) H_3^{(6^*)} \right) \\
 A_2 &= 0 \\
 B_1 &= -\frac{G}{\sqrt{2}} \chi_{\pm} f_c m_V^2 f_V \left(\frac{3}{2} (I_1 + I_2) (H_1^{(3^*)} + H_2^{(3^*)}) \right. \\
 &\quad \left. + \frac{1}{2} (I_1 - I_2) (H_1^{(6^*)} + H_2^{(6^*)}) \right) \\
 B_2 &= -\frac{G}{\sqrt{2}} \chi_{\pm} f_c m_V^2 f_V \frac{2}{M_1 + M_2} \left(\frac{3}{2} (I_1 + I_2) H_2^{(3^*)} + \frac{1}{2} (I_1 - I_2) H_2^{(6^*)} \right)
 \end{aligned} \tag{A 2}$$

In (A1) and (A2) the (+)-sign refers to decays involving a π^+ (S^+) and the (-)-sign to \bar{K}^0 (\bar{K}^{*0}). The pseudoscalar meson coupling constants are defined by

$$\langle \pi^+ | A_\mu | 0 \rangle = i f_{\pi^+} q_\mu \quad (\text{A } 3)$$

and correspondingly for \bar{K}^0 . The vector meson coupling constants are defined by

$$\langle S^+ | V_\mu | 0 \rangle = m_S^2 f_{S^+} g_{\mu a} e_a^* \quad (\text{A } 4)$$

and correspondingly for \bar{K}^{*0} . We use $f_{\pi^+} = 0.932 m_{\pi^+}$, $f_K = 1.28 f_{\pi^+}$, $f_{S^+} = 0.247$ and $f_{K^*} = f_{S^+}$. For the convenience of writing we have dropped explicit reference to the arguments of the form factors H_i .

As described in [31] the $q^2 = 0$ values of the various form factors H_i are fixed from the vector and axial vector form factors of known baryons. Following Buras [31] one has $H_1^{(6)}(0) = H_1^{(3^*)}(0) = 1$, $H_2^{(6)}(0) = -2.03$, $H_3^{(6)}(0) = -0.33$, $H_2^{(3^*)}(0) = 1.79$, $H_3^{(3^*)}(0) = 0.71$. We prefer to use the invariant form factors $H_i(q^2)$ to continue from $q^2 = 0$ to $q^2 = M_3^2$ as suggested in ref. [32,41] rather than the $G_E(q^2)$ and $G_M(q^2)$ as in ref. [31]. Continuation in terms of the latter form factors may be a doubtful procedure in the timelike region (see [42]). We use power behaved form factors of the form $\prod_{n=0}^{N-1} (1 - q^2/(m_{D^*}^2 + n\alpha'))^{-1}$ with $m_{D^*} = 2.006$ GeV, $m_{F^*} = 2.14$ GeV and a Regge slope $\alpha' = 0.25$ GeV⁻² as suggested by the $\Psi - \Psi'$ sequence. For H_1 and H_3 we take the canonical power behaviour $N = 2$ and for H_2 the canonical $N = 3$. Since nothing is known about the mass values of the even parity mesons

D_A and F_A that appear in the form factors H_3 we use the same mass values for these as for D^* and F^* .

In the case of decays involving a $3/2^+$ baryon the only decays with non-vanishing factorizing contribution are $T^0 \rightarrow \Xi^* \bar{K}^0 (\bar{K}^0)$ and $T^0 \rightarrow \Omega^- \pi^+ (S^+)$.

The vector and axial vector transition matrix elements that are needed for the evaluation of the factorizing contribution are obtained by relating them to the known $N-\Delta$ transition form factors [43]

One has for $1/2^+ \rightarrow 3/2^+ + 0^-$

$$A = 0$$

$$B = \frac{G}{\sqrt{2}} \chi_{\pm} f_c f_p I_1^* C_5^A \quad (A 5)$$

where $C_5^A(0) = -2.08$ from PCAC. The p.v. amplitude A is zero since the $1/2^+ \rightarrow 3/2^+$ vector transition is assumed to be conserved even for flavour changing transitions.

For $1/2^+ \rightarrow 3/2^+ + 1^-$ one has

$$A_1 = \frac{G}{\sqrt{2}} \chi_{\pm} f_c m_V^2 f_V I_1^* \frac{M_1 + M_2}{2M_2} C_5^A$$

$$A_2 = 0$$

$$A_3 = \frac{G}{\sqrt{2}} \chi_{\pm} f_c m_V^2 f_V I_1^* \frac{1}{M_2(M_1 + M_2)} C_5^A \quad (A 6)$$

and

$$B_1 = \frac{G}{\sqrt{2}} \chi_{\pm} f_c m_V^2 f_V I_1^* \frac{M_1 + M_2}{2M_2} \hat{C}_3^V$$

$$B_2 = M_2 B_1 / Q_+$$

$$B_3 = -B_1 / Q_+$$

(A 7)

For the p.c. amplitudes in (A7) we have assumed pure M_1 structure as is predicted in the quark model and is realized to a high degree in $N-\Delta$ photo transitions (see e.g. [42]). In (A5)-(A7) we have assumed SU(4) to hold for dimensionless invariants, where dimensions in the covariants are removed by multiplication with powers of $(M_1 + M_2)^{-1}$ as in [31]. In deriving (A7) we have used quark model results to relate the two nonzero axial vector $1/2^+ \rightarrow 3/2^+$ form factors [43]. Numerically $\hat{C}_3^V(0) = 8.25$ as follows from CVC [43]. Continuation from $q^2 = 0$ to $q^2 = M_3^2$ is achieved by using the above power behaved form factors with a power $N = 4$ [41]. Values for the tensor invariant I_1^* are listed in table 7.

Appendix B - Connection between Quark Model and Soft Pion Approach

The connection between the equal time commutator (ETC) term in the parity violating amplitude A of $1/2^+ \rightarrow 1/2^+ + 0^-$ that arises in the current algebra plus soft pion approach and the contributions of diagrams IIa and IIb in the quark model approach can be established by performing some tensor manipulations.

The ETC term has been worked out in (4.2) and is given by

$$A_{\alpha\beta\gamma}^{ETC} = -\frac{1}{f_P} \left(\langle B_\beta | Q_\gamma | B' \rangle \langle B' | \mathcal{X}_{p.c.} | B_\alpha \rangle - \langle B_\beta | \mathcal{X}_{p.c.} | B'' \rangle \langle B'' | Q_\gamma | B_\alpha \rangle \right) \quad (B 1)$$

where one sums over all intermediate $20'$ states B' and B'' that contribute to (B1).

We want to write (B1) in tensor notation. The tensor invariant for the matrix element $\langle B' | Q_\gamma | B \rangle$ is given by the antisymmetric invariant

$$\langle B' | Q_\gamma | B \rangle = (\bar{B}'^c [ab] - \bar{B}'^a [bc]) B_{c[db]} (Q_\gamma)_a^d \quad (B 2)$$

where $(Q_\gamma)_a^d$ is the normalized matrix representation of the generator Q_γ .

For the matrix element $\langle B' | \mathcal{X}_{p.c.} | B \rangle$ one has

$$\langle B' | \mathcal{X}_{p.c.} | B \rangle = a \bar{B}'^m [ke] B_{m[ij]} H_{[ke]}^{[ij]} \quad (B 3)$$

where a is the reduced matrix element of the coupling (B3). Note that there is only one $SU(4)$ coupling for (B3) since $20'$ occurs only once in the product

$$20' \otimes 20'' = \bar{4} + 20' + 36 + \bar{60} + 140' + 140'' \quad (B 4)$$

We can then rewrite A^{ETC} in the tensor representation and obtain

$$A_{\alpha\beta\gamma}^{ETC} = -\frac{a}{f_P} \left((Q_\gamma)_a^d (\bar{B}_\beta^c [ab] - \bar{B}_\beta^a [bc]) B_{c[db]} \bar{B}'^m [ke] B_{m[ij]} H_{[ke]}^{[ij]} \right. \\ \left. - \bar{B}_\beta^m [ke] B''^n [ij] H_{[ke]}^{[ij]} \bar{B}''^c [ab] (B_{c[db]}^\alpha - B_{d[bc]}^\alpha) (Q_\gamma)_\alpha^d \right) \quad (B 5)$$

where a summation over the 20' states B'_8 and B''_6 is understood.

We use the completeness relation for the sum over intermediate 20' states

$$\begin{aligned} \sum_{\alpha} \bar{B}_{\alpha}^{m[ke]} B_{c[db]}^{\alpha} &= \frac{2}{3} (\delta_c^m \delta_d^k \delta_b^e - \delta_c^m \delta_d^e \delta_b^k) \\ &+ \frac{1}{3} (\delta_d^m \delta_c^k \delta_b^e - \delta_d^m \delta_c^e \delta_b^k) \\ &- \frac{1}{3} (\delta_b^m \delta_c^k \delta_d^e - \delta_b^m \delta_c^e \delta_d^k) \end{aligned} \quad (B 6)$$

to rewrite (B5) and obtain

$$\begin{aligned} A_{\alpha\beta\gamma}^{ETC} &= -\frac{2\alpha}{f_P} \left(\bar{B}_{\beta}^{m[ae]} B_{m[ij]}^{\alpha} (Q_{\gamma})_a^k H_{[ke]}^{[ij]} + 2 \bar{B}_{\beta}^{k[ea]} B_{i[jm]}^{\alpha} (Q_{\gamma})_a^m H_{[ke]}^{[ij]} \right. \\ &\left. - \bar{B}_{\beta}^{m[ae]} B_{m[ij]}^{\alpha} (Q_{\gamma})_k^i H_{[ea]}^{[ki]} - 2 \bar{B}_{\beta}^{k[ea]} B_{i[jm]}^{\alpha} (Q_{\gamma})_a^m H_{[ke]}^{[ij]} \right) \end{aligned} \quad (B 7)$$

The first row in (B7) results from the first commutator term in (B1) where the SU(4) charge acts on the out state baryon, and the second row in (B7) results from the second commutator term in (B1) where the SU(4) charge acts on the in state baryon. As is required by CP invariance, the two terms corresponding to the contractions of fig. III cancel. The remaining terms in (B7) correspond to the tensor invariants I_3 and \hat{I}_3 which together form the correct CP combination $I_3^- = I_3 - \hat{I}_3$. Since latter invariant also determines the quark model contribution of figs. IIa and IIb in the symmetry limit (see 3.5) this proves our assertion of the group theoretical equivalence of the two approaches.

The above derivation is of course no proof of the dynamical equivalence of the ETC contribution and the contributions of the quark diagrams IIa and IIb. The result is, however, very suggestive of the existence of such an exact dynamical equivalence. If this were true this would be to our knowledge the first example where a soft pion result has its exact counterpart in the framework of the quark model.

Appendix C - Definitions of Amplitudes and Width Formulae

In order to clearly differentiate p.v. and p.c. amplitudes, the former will always be denoted by A_i and the latter by B_i . We shall also list the number of contributing LS amplitudes in each case, which we write as Γ_{LS} . For convenience of notation, we introduce the abbreviations $Q_{\pm} = P_1 P_2 \pm M_1 M_2$, where momenta and masses are labelled in the order $1 \rightarrow 2 + 3$. The c.m. momenta of the decay products are then $P_c = (Q_+ Q_-)^{1/2} / 2M_1$. We also use $k^2 = Q_- / Q_+$.

We shall define p.v. and p.c. helicity amplitudes by

$$H_{\lambda_1; \lambda_2 \lambda_3} \begin{matrix} \text{p.v.} \\ \text{p.c.} \end{matrix} = H_{\lambda_1; \lambda_2 \lambda_3} \pm H_{-\lambda_1; -\lambda_2 - \lambda_3} \quad (C 1)$$

The decay width is then given by

$$\Gamma = \frac{1}{8\pi M_1^2} \frac{P_c}{(2S_1 + 1)} \sum_{\text{hel. } (\lambda_1 > 0)} \frac{1}{2} (|H_{\lambda_1; \lambda_2 \lambda_3}^{\text{p.v.}}|^2 + |H_{\lambda_1; \lambda_2 \lambda_3}^{\text{p.c.}}|^2) \quad (C 2)$$

Case A: $1/2^+ \rightarrow 1/2^+ + 0^-$

LS-amplitudes: $\Gamma_{0, 1/2}^{\text{p.v.}}$; $\Gamma_{1, 1/2}^{\text{p.c.}}$

Invariant amplitudes: ($uu = 2m$)

$$\langle P_2 P_3 | \mathcal{L}_\omega(0) | P_1 \rangle = \bar{u}^2 (A + iB \gamma_5) u^1 \quad (C 3)$$

Helicity amplitudes:

$$H_{1/2; 1/2 0} \begin{matrix} \text{p.v.} \\ \text{p.c.} \end{matrix} = 2\sqrt{2} \begin{Bmatrix} \sqrt{Q_+} A \\ \sqrt{Q_-} B \end{Bmatrix} \quad (C 4)$$

Case B: $1/2^+ \rightarrow 1/2^+ + 1^-$

LS-amplitudes: $\Gamma_{0,1/2}^{P.V.}, \Gamma_{2,3/2}^{P.V.}; \Gamma_{1,1/2}^{P.C.}, \Gamma_{1,3/2}^{P.C.}$

Invariant amplitudes: $(e^\alpha e_\alpha = -1)$

$$\langle P_2 P_3 | \mathcal{H}_W(0) | P_1 \rangle = \bar{u}^2 e_\alpha^{*3} (A_1 i \gamma_\alpha \gamma_5 + A_2 P_{1a} i \gamma_5 + B_1 \gamma_\alpha + B_2 P_{1a}) \quad (C 5)$$

Helicity amplitudes:

$$H_{1/2; -1/2 -1} \begin{pmatrix} P.V. \\ P.C. \end{pmatrix} = 4 \begin{pmatrix} \sqrt{Q_+} A_1 \\ -\sqrt{Q_-} B_1 \end{pmatrix} \quad (C 6)$$

$$H_{1/2; 1/2 0} \begin{pmatrix} P.V. \\ P.C. \end{pmatrix} = \frac{2\sqrt{2}}{M_3} \begin{pmatrix} \sqrt{Q_+} (M_1 - M_2) A_1 - \sqrt{Q_-} M_1 p_c \cdot A_2 \\ \sqrt{Q_-} (M_1 + M_2) B_1 + \sqrt{Q_+} M_1 p_c \cdot B_2 \end{pmatrix}$$

Case C: $1/2^+ \rightarrow 3/2^+ + 0^-$

LS-amplitudes: $\Gamma_{2,3/2}^{P.V.}; \Gamma_{1,1/2}^{P.C.}$

Invariant amplitudes: $(\bar{u}_a u_a = 2m)$

$$\langle P_2 P_3 | \mathcal{H}_W(0) | P_1 \rangle = \bar{u}_a^2 (A P_{1a} i \gamma_5 + B P_{1a}) u^1 \quad (C 7)$$

Helicity amplitudes:

$$H_{1/2; 1/2 0} \begin{pmatrix} P.V. \\ P.C. \end{pmatrix} = 4 \sqrt{1/3} p_c (M_1/M_2) \begin{pmatrix} \sqrt{Q_-} A \\ \sqrt{Q_+} B \end{pmatrix} \quad (C 8)$$

For the inverse process $3/2^+ \rightarrow 1/2^+ + 0^-$ one defines

$$\langle P_2 P_3 | \mathcal{R}_W(0) | P_1 \rangle = \bar{u}^2 (A P_{2a} i\delta_5 + B P_{2a}) u^1_a \quad (C9)$$

with

$$H_{1/2; 1/2 0} \left\{ \begin{array}{c} \text{P.V.} \\ \text{P.C.} \end{array} \right\} = 4 \sqrt{\frac{1}{3}} P_C \left\{ \begin{array}{c} \sqrt{Q_-} A \\ \sqrt{Q_+} B \end{array} \right\} \quad (C10)$$

Case D: $1/2^+ \rightarrow 3/2^+ + 1^-$

LS-amplitudes: $\Gamma_{0, 1/2}^{\text{P.V.}}, \Gamma_{2, 3/2}^{\text{P.V.}}, \Gamma_{2, 5/2}^{\text{P.V.}}; \Gamma_{1, 1/2}^{\text{P.C.}}, \Gamma_{1, 3/2}^{\text{P.C.}}, \Gamma_{3, 5/2}^{\text{P.C.}}$

Invariant amplitudes

$$\begin{aligned} \langle P_2 P_3 | \mathcal{R}_W(0) | P_1 \rangle = \bar{u}_a e_b^{*3} (& A_1 g_{ab} + A_2 P_{1a} \delta_b + A_3 P_{1a} P_{1b} \\ & + B_1 g_{ab} i\delta_5 + B_2 P_{1a} \delta_5 i\delta_5 + B_3 P_{1a} P_{1b} i\delta_5) u^1 \quad (C11) \end{aligned}$$

Helicity amplitudes:

$$H_{1/2; 3/2 1} \left\{ \begin{array}{c} \text{P.V.} \\ \text{P.C.} \end{array} \right\} = 2\sqrt{2} \left\{ \begin{array}{c} \sqrt{Q_+} A_1 \\ \sqrt{Q_-} B_1 \end{array} \right\}$$

$$H_{1/2; -1/2 -1} \left\{ \begin{array}{c} \text{P.V.} \\ \text{P.C.} \end{array} \right\} = 2\sqrt{2/3} \left\{ \begin{array}{c} \sqrt{Q_+} (A_1 - 2Q_-/M_2 A_2) \\ -\sqrt{Q_-} (B_1 - 2Q_+/M_2 B_2) \end{array} \right\} \quad (C12)$$

$$H_{1/2; 1/2 0} \left\{ \begin{array}{c} \text{P.V.} \\ \text{P.C.} \end{array} \right\} = \frac{4}{\sqrt{3} M_2 M_3} \left\{ \begin{array}{c} \sqrt{Q_+} (\frac{1}{2} (M_1^2 - M_2^2 - M_3^2) A_1 + Q_- (M_1 + M_2) A_2 + M_1^2 P_C^2 A_3) \\ -\sqrt{Q_-} (\frac{1}{2} (M_1^2 - M_2^2 - M_3^2) B_1 - Q_+ (M_1 - M_2) B_2 + M_1^2 P_C^2 B_3) \end{array} \right\}$$

It is convenient to introduce also transverse multipole amplitudes:

$$\begin{aligned} M1 &= \frac{1}{2} (H_{1/2; -1/2 -1}^{\text{P.C.}} + \sqrt{3} H_{1/2; 3/2 1}^{\text{P.C.}}) \\ E2 &= \frac{1}{\sqrt{12}} (3 H_{1/2; -1/2 -1}^{\text{P.C.}} - \sqrt{3} H_{1/2; 3/2 1}^{\text{P.C.}}) \end{aligned} \quad (C13)$$

$$\begin{aligned} E1 &= \frac{1}{2} (- H_{1/2; -1/2 -1}^{\text{P.V.}} - \sqrt{3} H_{1/2; 3/2 1}^{\text{P.V.}}) \\ M2 &= \frac{1}{\sqrt{12}} (3 H_{1/2; -1/2 -1}^{\text{P.V.}} - \sqrt{3} H_{1/2; 3/2 1}^{\text{P.V.}}) \end{aligned}$$

References

1. Piccolo M. et al.: Phys. Rev. Lett. 39, 1503 (1977)
2. Ferguson T. et al.: SLAC PUB 2081 (1978)
3. Cazzoli E.G. et al.: Phys. Rev. Lett. 34, 1125 (1975)
4. Knapp B. et al.: Phys. Rev. Letters 37, 882 (1976)
5. Glashow S.L., Iliopoulos J., Maiani L.: Phys. Rev. D2, 1285 (1970)
6. Körner J.G., Kramer G., Willrodt J.: Phys. Lett. B (to be published)
and DESY Preprint 78/13
7. Quigg C., Rosner J.L.: Fermilab-Pub-77/60-THY (1977)
8. Scharre D.L. et al.: Phys. Rev. Lett. 40, 74 (1977)
9. Lee B.W., Gaillard M.K.: Phys. Rev. Lett. 33, 108 (1974);
Altarelli G., Maiani L.: Phys. Lett. 52B, 351 (1974)
10. Lee B.W., Quigg C., Rosner J.L.: Phys. Rev. D15, 157 (1977)
11. De Rujula A., Georgi H., Glashow S.L.: Phys. Rev. D12, 147 (1975)
12. Wilson K., Phys. Rev. 179, 1499 (1969)
13. Ellis J., Gaillard M.K., Nanopoulos D.V.: Nuclear Physics B100,
313 (1975)
14. Nanopoulos D.V.: in Current Induced Reactions, Eds. J.G. Körner,
G. Kramer and D. Schildknecht, Springer, Heidelberg
15. Cabibbo N., Maiani L.: Phys. Lett. 73B, 418 (1978)

16. Ellis J., Gaillard M.K., Nanopoulos D.V., Rudaz S.:
Nucl. Phys. B131, 285 (1977)
17. Altarelli G., Cabibbo N., Maiani L.: Phys. Lett. 57B, 277 (1975)
18. Rubinstein H.R., Stodolsky L., Wagner F., Wolff U.: Phys. Lett. 73B,
433 (1978)
19. Kazi A., Kramer G., Schiller D.H.: Acta Phys. Austr. 45, 195 (1976)
20. Haacke E.M., Moffat J.W., Savaria P.: J. Math. Phys. 17, 2041 (1976)
Rabl V., Campbell Jr. G., Wali K.C.: J. Math. Phys. 16, 2494 (1975)
21. Iwasaki Y.: Phys. Rev. Lett. 34, 1407 (1975); (E) ibid 35, 264 (1975)
22. Kobayashi M., Nakogawa M., Nitto H.: Prog. Theor. Phys. 47, 982 (1972)
23. Körner J.G.: Nucl. Phys. 25B, 282 (1970)
24. Miura K., Minakawa T.: Progr. Theor. Phys. 38, 954 (1967)
Pati J.C., Woo C.H.: Phys. Rev. D3, 2920 (1971)
25. Fakirov D., Stech B.: Nucl. Phys. B133, 315 (1978)
26. Delbourgo R., Salam A., Strathdee J.: Proc. Roy. Soc. A 278, 146 (1965);
Gudehus T., DESY Report 68/11 (1968) unpublished;
Phys. Rev. 184, 1788 (1969)
27. Craigie N.S., Jones H.F., Milani P.: Imperial College Preprint
ICTP/77-78/12 (1978); Ali A., Körner J.G., Kramer G., Willrodt J.:
DESY Preprint 78/51 (to be published)
28. Maiani L.: INFN Preprint, Rome (1978)
29. Körner J.G., Kramer G., Willrodt J.: DESY Preprint 78/ (1978)

30. Körner J.G., Gudehus T.: Nuovo Cimento 11A, 597 (1972)
31. Buras A.J.: Nuclear Physics B109, 373 (1976)
32. Avilez C., Kobayashi H., Körner J.G.: Phys. Rev. D17, 709 (1978)
33. Bourquin M. et al.: CERN Preprint (1978)
34. Cortéz J.L., Morales A., Nuñez-Lagos R., Sánchez-Guillén J.:
Zaragoza Preprint IFNAE 1/78
35. Gronau M.: Phys. Rev. Lett. 28, 188 (1972); Phys. Rev. D5, 118 (1972)
36. Shifman M.A., Vainshtein A.I., Zakharov V.I.: Nucl. Phys. B120, 316
(1977); ITEP Preprints ITEP-63 and 64 (1976)
37. Finjord J.: CERN Preprint 2452 (1978)
38. Particle Data Group, Phys. Letters 75B, (1978)
39. Brown L.S., Sommerfield C.M.: Phys. Rev. Lett. 16, 751 (1966); Hara Y.,
Nambu Y., Schechter J.: Phys. Rev. Lett 16, 380 (1966)
40. Lee B.W.: Phys. Rev. 170, 1359 (1968); Schechter J.: Phys. Rev. 174,
1829 (1968)
41. Devenish R.C.E., Eisenschitz T.S., Körner J.G.: Phys. Rev. D14, 3063
(1976); Körner J.G., Kuroda M.: Phys. Rev. D16, 2165 (1977)
42. Körner J.G., Kuroda M.: Phys. Lett. 67B, 455 (1977)
43. Körner J.G., Kobayashi H., Avilez C.: DESY Preprint 77/23

Table 1: Charmed $1/2^+$ baryon states. $[ab]$ and $\{ab\}$ denote antisymmetric and symmetric flavour index combinations.

notation	quark content	SU(3)	(I, I ₃)	S	C	mass (GeV)
C_0^+	$c[u,d]$	$\bar{3}$	(0,0)	0	1	2.26
A^+	$c[s,u]$	$\bar{3}$	(1/2,1/2)	-1	1	2.47
A^0	$c[s,d]$	$\bar{3}$	(1/2,-1/2)	-1	1	2.47
C_1^{++}	cuu	6	(1,1)	0	1	2.42
C_1^+	$c\{u,d\}$	6	(1,0)	0	1	2.42
C_1^0	cdd	6	(1,-1)	0	1	2.42
S^+	$c\{s,u\}$	6	(1/2,1/2)	-1	1	2.56
S^0	$c\{s,d\}$	6	(1/2,-1/2)	-1	1	2.56
T^0	css	6	(0,0)	-2	1	2.73
X_u^{++}	ccu	3	(1/2,1/2)	0	2	3.61
X_d^+	ccd	3	(1/2,-1/2)	0	2	3.61
X_s^+	ccs	3	(0,0)	-1	2	3.79

Table 2: Charmed $3/2^+$ baryon states

notation	quark content	SU(3)	(I, I_3)	S	C	mass (GeV)
C_1^{*++}	cuu	6	(1,1)	0	1	2.49
C_1^{*+}	cud	6	(1,0)	0	1	2.49
C_1^{*0}	cdd	6	(1,-1)	0	1	2.49
S^{*+}	cus	6	(1/2,1/2)	-1	1	2.61
S^{*0}	cds	6	(1/2,-1/2)	-1	1	2.61
T^{*0}	css	6	(0,0)	-2	1	2.77
X_u^{*++}	ccu	3	(1/2,1/2)	0	2	3.67
X_d^{*+}	ccd	3	(1/2,-1/2)	0	2	3.67
X_s^{*+}	ccs	3	(0,0)	-1	2	3.85
Θ^{++}	ccc	1	(0,0)	0	3	4.89

Table 3: Flavour content of charm changing interaction

decay	amplitude	ΔS	ΔI
$c \rightarrow s\bar{d}$	$\cos^2\theta_c$	1	+1
$c \rightarrow d\bar{d}$	$-\cos\theta_c \sin\theta_c$	0	1/2, 3/2
$c \rightarrow s\bar{s}$	$\cos\theta_c \sin\theta_c$	0	1/2
$c \rightarrow d\bar{s}$	$-\sin^2\theta_c$	-1	0, 1

Table 4a: I, U and V spin multiplets for mesons

I-spin	
s = singlets:	$\eta_8; \eta_{15}; F^+; F^-$
d = doublets:	$K^+, K^0; \bar{K}^0, -K^-; \bar{D}^0, D^-; D^+, -D^0$
t = triplets:	$-\pi^+, \pi^0, \pi^-$
U-spin	
s:	$\eta_{15}; D^0; \bar{D}^0; (\eta_8 + \sqrt{3}\pi^0)/2$
d:	$\pi^-, K^-; K^+, -\pi^+; D^-, F^-; F^+, -D^+$
t:	$-K^0, (\sqrt{3}\eta_8 - \pi^0)/2, \bar{K}^0$
V-spin	
s:	$\eta_{15}; (\sqrt{3}\pi^0 - \eta_8)/2; D^+; D^-$
d:	$\bar{D}^0, F^-; F^+, -D^0; \pi^+, \bar{K}^0; K^0, -\pi^-$
t:	$-K^+, (\pi^0 + \sqrt{3}\eta_8)/2, K^-$

Table 4b: I, U and V spin multiplets for J= 1/2 baryons

I-spin	
s:	$\Lambda; C_0^+; T^0; X_s^+$
d:	$p, n; \Xi^0, -\Xi^-; S^+, S^0; A^+, A^0; X_u^{++}, X_d^+$
t:	$\Sigma^+, \Sigma^0, -\Sigma^-; C_1^{++}, C_1^+, C_1^0$
U-spin	
s:	$(\Lambda - \sqrt{3}\Sigma^0)/2; A^0; X_u^{++}; C_1^{++}$
d:	$p, \Sigma^+; \Sigma^-, \Xi^-; C_0^+, A^+; X_d^+, X_s^+; C_1^+, S^+$
t:	$n, (\sqrt{3}\Lambda + \Sigma^0)/2, \Xi^0; C_1^0, S^0, T^0$
V-spin	
s:	$(\Lambda - \sqrt{3}\Sigma^0)/2; A^+; X_d^+; C_1^0$
d:	$n, \Sigma^-; \Sigma^+, \Xi^0; C_0^+, A^0; X_u^{++}, X_s^+; C_1^+, S^0$
t:	$p, (\sqrt{3}\Lambda + \Sigma^0)/2, \Xi^-; C_1^{++}, S^+, T^0$

Table 4c: I, U and V spin multiplets for J=3/2 baryons

	I-spin
s:	$\Omega^-; R^{*++}; T^{*0}; X_s^{*+}$
d:	$\Xi^{*0}, \Xi^{*-}; S^{*+}, S^{*0}; X_u^{*++}, X_d^{*+}$
t:	$\Sigma^{*+}, \Sigma^{*0}, \Sigma^{*-}; C_1^{*++}, C_1^{*+}, C_1^{*0}$
q:	$\Delta^{++}, \Delta^+, \Delta^0, \Delta^-$
	U-spin
s:	$\Delta^{++}; R^{*++}; C_1^{*++}; X_u^{*++}$
d:	$\Delta^+, \Sigma^{*+}; C_1^{*+}, S^{*+}; X_d^{*+}, X_s^{*+}$
t:	$\Delta^0, \Sigma^{*0}, \Xi^{*0}; C_1^{*0}, S^{*0}, T^{*0}$
q:	$\Delta^-, \Sigma^{*-}, \Xi^{*-}, \Omega^-$
	V-spin
s:	$\Delta^-; R^{*++}; C_1^{*0}; X_d^{*+}$
d:	$\Delta^0, \Sigma^{*-}; C_1^{*+}, S^{*0}; X_u^{*++}, X_s^{*+}$
t:	$\Delta^+, \Sigma^{*0}, \Xi^{*-}; C_1^{*++}, S^{*+}, T^{*0}$
q:	$\Delta^{++}, \Sigma^{*+}, \Xi^{*0}, \Omega^-$

Table 5 : I, U and V spin sumrules

a) From $\Delta I = 1$ property

$$(C_0^+ \rightarrow \Sigma^+ \pi^0) = - (C_0^+ \rightarrow \Sigma^0 \pi^+)$$

$$(A^0 \rightarrow \Xi^- \pi^+) + \sqrt{2} (A^0 \rightarrow \Xi^0 \pi^0) = - (A^+ \rightarrow \Xi^0 \pi^+)$$

$$(A^0 \rightarrow \Sigma^+ K^-) + \sqrt{2} (A^0 \rightarrow \Sigma^0 \bar{K}^0) = - (A^+ \rightarrow \Sigma^+ \bar{K}^0)$$

$$(C_0^+ \rightarrow \Delta^{++} K^-) = \sqrt{3} (C_0^+ \rightarrow \Delta^+ \bar{K}^0)$$

$$(C_0^+ \rightarrow \Sigma^{*+} \pi^0) = (C_0^+ \rightarrow \Sigma^{*0} \pi^+)$$

$$(A^0 \rightarrow \Xi^{*-} \pi^+) + \sqrt{2} (A^0 \rightarrow \Xi^{*0} \pi^0) = - (A^+ \rightarrow \Xi^{*0} \pi^+)$$

$$(A^0 \rightarrow \Sigma^{*+} K^-) - \sqrt{2} (A^0 \rightarrow \Sigma^{*0} \bar{K}^0) = - (A^+ \rightarrow \Sigma^{*+} \bar{K}^0)$$

b) From $\Delta U = 1$ property

$$(A^0 \rightarrow \Xi^0 \pi^0) + (A^0 \rightarrow \Sigma^0 \bar{K}^0) = \sqrt{3} (A^0 \rightarrow \Lambda \bar{K}^0) + \sqrt{3} (A^0 \rightarrow \Xi^0 \eta_8)$$

$$\sqrt{2} (C_0^+ \rightarrow \Xi^0 K^+) - \sqrt{3} (C_0^+ \rightarrow \Lambda \pi^+) + (C_0^+ \rightarrow \Sigma^0 \pi^+) = \sqrt{2} (A^+ \rightarrow \Xi^0 \pi^+)$$

$$\sqrt{3} (C_0^+ \rightarrow \Sigma^+ \eta_8) - (C_0^+ \rightarrow \Sigma^+ \pi^0) - \sqrt{2} (C_0^+ \rightarrow \rho \bar{K}^0) = -\sqrt{2} (A^+ \rightarrow \Sigma^+ \bar{K}^0)$$

$$2 (A^0 \rightarrow \Sigma^{*0} \bar{K}^0) = -\sqrt{3} (A^0 \rightarrow \Xi^{*0} \eta_8) + (A^0 \rightarrow \Xi^{*0} \pi^0)$$

$$(C_0^+ \rightarrow \Xi^{*0} K^+) - \sqrt{2} (C_0^+ \rightarrow \Sigma^{*0} \pi^+) = (A^+ \rightarrow \Xi^{*0} \pi^+)$$

$$\sqrt{3} (C_0^+ \rightarrow \Sigma^{*+} \eta_8) - (C_0^+ \rightarrow \Sigma^{*+} \pi^0) - \sqrt{2} (C_0^+ \rightarrow \Delta^+ \bar{K}^0) = -\sqrt{2} (A^+ \rightarrow \Sigma^{*+} \bar{K}^0)$$

c) From $\Delta V = 0$ property of 0^-

$$(C_0^+ \rightarrow \Sigma^0 \pi^+) + \sqrt{3} (C_0^+ \rightarrow \Lambda \pi^+) - \sqrt{2} (C_0^+ \rightarrow \rho \bar{K}^0) = 0$$

$$(C_0^+ \rightarrow \Sigma^+ \pi^0) + \sqrt{3} (C_0^+ \rightarrow \Sigma^+ \eta_8) - \sqrt{2} (C_0^+ \rightarrow \Xi^0 K^+) = 0$$

$$(A^0 \rightarrow \Xi^0 \pi^0) + \sqrt{3} (A^0 \rightarrow \Xi^0 \eta_8) + \sqrt{2} (A^0 \rightarrow \Sigma^+ K^-) = 0$$

$$(C_0^+ \rightarrow \Xi^0 K^+) + (A^0 \rightarrow \Sigma^+ K^-) = 0$$

$$(A^0 \rightarrow \Sigma^0 \bar{K}^0) + \sqrt{3} (A^0 \rightarrow \Lambda \bar{K}^0) + \sqrt{2} (A^0 \rightarrow \Xi^- \pi^+) = 0$$

$$(C_0^+ \rightarrow \rho \bar{K}^0) + (A^0 \rightarrow \Xi^- \pi^+) = 0$$

$$\sqrt{2} (C_0^+ \rightarrow \Sigma^+ \pi^0) - (C_0^+ \rightarrow \Xi^0 K^+) + \sqrt{2} (A^0 \rightarrow \Xi^0 \pi^0) = 0$$

$$(A^+ \rightarrow \Xi^0 \pi^+) + (A^+ \rightarrow \Sigma^+ \bar{K}^0) = 0$$

$$(C_0^+ \rightarrow \Delta^+ \bar{K}^0) + \sqrt{2} (C_0^+ \rightarrow \Sigma^{*0} \pi^+) = 0$$

$$(C_0^+ \rightarrow \Delta^+ \bar{K}^0) + (A^0 \rightarrow \Xi^{*-} \pi^+) = 0$$

$$(C_0^+ \rightarrow \Delta^+ \bar{K}^0) - \sqrt{2} (A^0 \rightarrow \Sigma^{*0} \bar{K}^0) = 0$$

$$(A^+ \rightarrow \Sigma^{*+} \bar{K}^0) = (A^+ \rightarrow \Xi^{*0} \pi^+) = 0$$

$$(C_0^+ \rightarrow \Sigma^{*+} \eta_8) - \sqrt{3} (C_0^+ \rightarrow \Sigma^{*+} \pi^0) = 0$$

$$(A^0 \rightarrow \Xi^{*0} \eta_8) + \sqrt{3} (A^0 \rightarrow \Xi^{*0} \pi^0) = 0$$

$$(C_0^+ \rightarrow \Delta^{*+} K^-) - \sqrt{3} (C_0^+ \rightarrow \Xi^{*0} K^+) = 0$$

$$(C_0^+ \rightarrow \Delta^{*+} K^-) + (A^0 \rightarrow \Omega^- K^+) = 0$$

$$\sqrt{3} (T^0 \rightarrow \Xi^{*0} \bar{K}^0) - (T^0 \rightarrow \Omega^- \pi^+) = 0$$

d) From $\Delta V = 1$ property of 0^+

$$(A^+ \rightarrow \Sigma^+ \bar{K}^0) - (A^+ \rightarrow \Xi^0 \pi^+) = 0$$

$$(C_0^+ \rightarrow p \bar{K}^0) + (A^0 \rightarrow \Xi^- \pi^+) = 0$$

$$(C_0^+ \rightarrow \Xi^0 K^+) + (A^0 \rightarrow \Sigma^+ K^-) = 0$$

$$2(C_0^+ \rightarrow \Lambda \pi^+) - (A^0 \rightarrow \Lambda \bar{K}^0) - \sqrt{3}(A^0 \rightarrow \Sigma^0 \bar{K}^0) = 0$$

$$2(C_0^+ \rightarrow \Sigma^0 \pi^+) - \sqrt{3}(A^0 \rightarrow \Lambda K^0) + (A^0 \rightarrow \Sigma^0 \bar{K}^0) = 0$$

$$2(C_0^+ \rightarrow \Sigma^+ \pi^0) + (A^0 \rightarrow \Xi^0 \pi^0) - \sqrt{3}(A^0 \rightarrow \Xi^0 \eta_8) = 0$$

$$2(C_0^+ \rightarrow \Sigma^+ \eta_8) - \sqrt{3}(A^0 \rightarrow \Xi^0 \pi^0) - (A^0 \rightarrow \Xi^0 \eta_8) = 0$$

$$(C_0^+ \rightarrow \Delta^+ \bar{K}^0) - (A^0 \rightarrow \Xi^{*-} \pi^+) = 0$$

$$(C_0^+ \rightarrow \Sigma^{*0} \pi^+) - (A^0 \rightarrow \Sigma^{*0} \bar{K}^0) = 0$$

$$(A^+ \rightarrow \Sigma^{*+} \bar{K}^0) + (A^+ \rightarrow \Xi^{*0} \pi^+) = 0$$

$$(C_0^+ \rightarrow \Xi^{*0} K^+) - (A^0 \rightarrow \Sigma^{*+} K^-) = 0$$

$$(C_0^+ \rightarrow \Delta^{++} K^-) - (A^0 \rightarrow \Omega^- K^+) = 0$$

$$(C_0^+ \rightarrow \Sigma^{*+} \pi^0) - (A^0 \rightarrow \Xi^{*0} \pi^0) = 0$$

$$(C_0^+ \rightarrow \Sigma^{*+} \eta_8) - (A^0 \rightarrow \Xi^{*0} \eta_8) = 0$$

$$\sqrt{6}(C_0^+ \rightarrow \Sigma^{*+} \pi^0) + 3\sqrt{2}(C_0^+ \rightarrow \Sigma^{*+} \eta_8) + 2(C_0^+ \rightarrow \Delta^{++} K^-) - 2\sqrt{3}(C_0^+ \rightarrow \Xi^{*0} K^+) = 0$$

Table 6:

	I_1	I_2	I_3	I_4	\hat{I}_3	\hat{I}_4	I_5
$6 C_6^+ \rightarrow \Lambda \pi^+$	-2	-2	-2	+4	-2	+4	+1
$\sqrt{12} C_6^+ \rightarrow \Sigma^0 \pi^+$	0	0	-2	0	+2	-4	-1
$\sqrt{12} C_6^+ \rightarrow \Sigma^+ \pi^0$	0	0	+2	0	-2	+4	+1
$6 C_6^+ \rightarrow \Sigma^+ \eta_8$	0	0	-2	+4	+2	-4	+1
$\sqrt{18} C_6^+ \rightarrow \Sigma^+ \eta_1$	0	0	+4	-2	+2	-4	+1
$\sqrt{6} C_6^+ \rightarrow \rho \bar{K}^0$	-1	-1	-2	+2	0	0	0
$\sqrt{6} C_6^+ \rightarrow \Xi^0 K^+$	0	0	0	+2	0	0	+1
$\sqrt{6} A^+ \rightarrow \Sigma^+ \bar{K}^0$	-1	-1	0	0	-2	4	0
$\sqrt{6} A^+ \rightarrow \Xi^0 \pi^+$	1	1	0	0	2	-4	0
$6 A^0 \rightarrow \Lambda \bar{K}^0$	1	1	4	-2	-2	4	1
$\sqrt{12} A^0 \rightarrow \Sigma^0 \bar{K}^0$	1	1	0	-2	2	-4	-1
$\sqrt{6} A^0 \rightarrow \Sigma^+ K^-$	0	0	0	2	0	0	1
$\sqrt{12} A^0 \rightarrow \Xi^0 \pi^0$	0	0	2	-2	-2	4	0
$6 A^0 \rightarrow \Xi^0 \eta_8$	0	0	-2	-2	2	-4	-2
$\sqrt{18} A^0 \rightarrow \Xi^0 \eta_1$	0	0	4	-2	2	-4	1
$\sqrt{6} A^0 \rightarrow \Xi^- \pi^+$	-1	-1	-2	2	0	0	0
$T^0 \rightarrow \Xi^0 \bar{K}^0$	1	-1	0	0	2	0	0
$\sqrt{6} \Lambda \rightarrow \rho \pi^-$	-1	-1	0	2	-2	4	1
$\sqrt{12} \Lambda \rightarrow n \pi^0$	1	1	0	-2	2	-4	-1
$\sqrt{2} \Sigma^+ \rightarrow \rho \pi^0$	1	-1	0	2	2	0	1
$\Sigma^+ \rightarrow n \pi^+$	0	0	0	2	0	0	1
$\Sigma^- \rightarrow n \pi^-$	-1	1	0	0	-2	0	0
$\sqrt{6} \Xi^- \rightarrow \Lambda \pi^-$	2	-1	0	0	4	-4	0
$\sqrt{12} \Xi^0 \rightarrow \Lambda \pi^0$	2	1	0	0	-4	4	0

Table 6 (Caption)

Values of SU(4) invariants for ground state $1/2^+$ baryons. Note the identity $2I_1 = (I_3 + \hat{I}_3)$. Further identities hold for SU(4) subspaces, as e.g. $I_1 = I_2$ and $\hat{I}_4 = -2\hat{I}_3$ for C_0^+ , A^+ and A^0 decays. The η_8 appearing in the table is the unphysical $I = 0, Y = 0$ SU(3) octet state. We have also included values of the tensor invariants for the unphysical SU(3) singlet state η_1 . The corresponding values for the physical states η and η' are obtained from the linear combinations

$$\sqrt{6}\eta = (1+\sqrt{2})\eta_8 - (1-\sqrt{2})\eta_1 \quad \text{and} \quad \sqrt{6}\eta' = (1-\sqrt{2})\eta_8 + (1+\sqrt{2})\eta_1.$$

Similarly the appropriate combinations for the physical states ω and Ψ

$$\text{(using ideal mixing) are } \Psi = -\sqrt{2/3}\eta_8 + \sqrt{1/3}\eta_1 \quad \text{and} \quad \omega = \sqrt{1/3}\eta_8 + \sqrt{2/3}\eta_1.$$

We have always factored out the product of flavour space quark model wave function normalizations.

	$I_1^{*\pm}$	$I_2^{*\pm}$		$I_1^{*\pm}$	$I_2^{*\pm}$
$6 C_0^+ \rightarrow \Sigma^{*0} \pi^+$	0	2	$6 A^0 \rightarrow \Sigma^{*0} \bar{K}^0$	0	-2
$6 C_0^+ \rightarrow \Sigma^{*+} \pi^0$	0	2	$\sqrt{18} A^0 \rightarrow \Sigma^{*+} K^-$	0	-2
$\sqrt{108} C_0^+ \rightarrow \Sigma^{*+} \eta_8$	0	6	$6 A^0 \rightarrow \Xi^{*0} \pi^0$	0	-2
$\sqrt{54} C_0^+ \rightarrow \Sigma^{*+} \eta_1$	0	0	$\sqrt{108} A^0 \rightarrow \Xi^{*0} \eta_8$	0	2
$\sqrt{18} C_0^+ \rightarrow \Delta^{*+} \bar{K}^0$	0	-2	$\sqrt{54} A^0 \rightarrow \Xi^{*0} \eta_1$	0	-4
$\sqrt{6} C_0^+ \rightarrow \Delta^{*+} K^-$	0	-2	$\sqrt{18} A^0 \rightarrow \Xi^{*-} \pi^+$	0	2
$\sqrt{18} C_0^+ \rightarrow \Xi^{*0} K^+$	0	2	$\sqrt{6} A^0 \rightarrow \Omega^- K^+$	0	2
$\sqrt{18} A^+ \rightarrow \Sigma^{*+} \bar{K}^0$	0	0	$\sqrt{3} T^0 \rightarrow \Xi^{*0} \bar{K}^0$	-1	0
$\sqrt{18} A^+ \rightarrow \Xi^{*0} \pi^+$	0	0	$T^0 \rightarrow \Omega^- \pi^+$	-1	0
$\Omega^- \rightarrow \Xi^0 \pi^-$	± 1	0			
$\sqrt{2} \Omega^- \rightarrow \Xi^- \pi^0$	± 1	0			
$\sqrt{6} \Omega^- \rightarrow \Lambda K^-$	0	± 4			

Table 7:

Values of SU(4) invariants for ground state ($1/2^+ \rightarrow 3/2^+ + \text{meson}$) transitions. Further explanation as in caption of table 6.

	Quark Model		SU(4)		Current Algebra	
	Γ	α	Γ	α	Γ	α
$C_0^+ \rightarrow \Lambda \pi^+$	0.08	0.86	0.28	0.0	0.38	-1.0
$C_0^+ \rightarrow \Sigma^0 \pi^+$	0.09	-0.99	0.05	-0.76	0.55	-0.97
$C_0^+ \rightarrow \Sigma^+ \pi^0$	0.09	-1.00	0.05	-0.76	0.55	-0.97
$C_0^+ \rightarrow \Sigma^+ \eta$	0.27	-0.96	-	-	-	-
$C_0^+ \rightarrow \Sigma^+ \eta'$	0.35	-0.88	-	-	-	-
$C_0^+ \rightarrow \rho \bar{K}^0$	0.89	-0.68	0.63	-0.34	0.16	-0.88
$C_0^+ \rightarrow \Xi^0 K^+$	0.22	0.0	0.07	+0.01	0.00	0.0
$A^+ \rightarrow \Sigma^+ \bar{K}^0$	0.98	-0.86	0.04	+1.00	0.62	-0.94
$A^+ \rightarrow \Xi^0 \pi^+$	0.08	-0.96	0.04	+1.00	1.23	+0.64
$A^0 \rightarrow \Lambda \bar{K}^0$	0.27	-1.00	0.17	-0.77	0.20	-0.97
$A^0 \rightarrow \Sigma^0 \bar{K}^0$	0.39	0.38	0.16	+0.49	0.08	-0.63
$A^0 \rightarrow \Sigma^+ K^-$	0.43	0.0	0.17	+0.06	0.26	-0.22
$A^0 \rightarrow \Xi^0 \pi^0$	0.08	0.92	0.19	-0.85	1.28	-0.90
$A^0 \rightarrow \Xi^0 \eta$	0.18	0.95	-	-	0.03	0.0
$A^0 \rightarrow \Xi^0 \eta'$	0.79	-0.97	-	-	-	-
$A^0 \rightarrow \Xi^- \pi^+$	0.24	-0.03	0.48	-0.42	0.89	+0.50
$T^0 \rightarrow \Xi^0 \bar{K}^0$	6.87	0.38	0.11	-0.19	1.42	-0.98

Table 8:

Partial width (in units of 10^{12} sec^{-1}) and asymmetry α for $1/2^+ \rightarrow 1/2^+ + 0^-$ in the quark model, SU(4) and in the current algebra approach. Our asymmetry α is defined such that $\alpha_{\Lambda \rightarrow \rho \pi^-}^{\text{exp}}$ is positive.

Table 9: Partial widths for decays $1/2^+ \rightarrow 3/2^+ + 0^-$ (in units of 10^{12} sec^{-1}).

Second and fifth column: this quark model calculation. X denotes kinematically forbidden processes. Third and sixth column: SU(4) result normalized to $\Omega^- \rightarrow \Lambda K^-$. Because of η - η' mixing there are no SU(4) predictions for η -decays. T^0 decays are not related to $\Omega^- \rightarrow \Lambda K^-$ (see text).

	Q.M.	SU(4)		Q.M.	SU(4)
$C_0^+ \rightarrow \Sigma^{*0} \pi^+$	0.23	0.17	$A^0 \rightarrow \Sigma^{*0} \bar{K}^0$	0.31	0.20
$C_0^+ \rightarrow \Sigma^{*+} \pi^0$	0.23	0.17	$A^0 \rightarrow \Sigma^{*+} K^-$	0.63	0.41
$C_0^+ \rightarrow \Sigma^{*+} \eta$	0.31	-	$A^0 \rightarrow \Xi^{*0} \pi^0$	0.29	0.18
$C_0^+ \rightarrow \Sigma^{*+} \eta'$	X	X	$A^0 \rightarrow \Xi^{*0} \eta$	0.01	-
$C_0^+ \rightarrow \Delta^+ \bar{K}^0$	0.51	0.41	$A^0 \rightarrow \Xi^{*0} \eta'$	X	X
$C_0^+ \rightarrow \Delta^{*+} K^-$	1.54	1.23	$A^0 \rightarrow \Xi^{*-} \pi^+$	0.57	0.35
$C_0^+ \rightarrow \Xi^{*0} K^+$	0.11	0.07	$A^0 \rightarrow \Omega^- K^+$	0.62	0.36
$A^+ \rightarrow \Sigma^{*+} \bar{K}^0$	0.0	0.0	$T^0 \rightarrow \Xi^{*0} \bar{K}^0$	0.01	-
$A^+ \rightarrow \Xi^{*0} \pi^+$	0.0	0.0	$T^0 \rightarrow \Omega^- \pi^+$	1.02	-

Table 10: Partial widths for decays $1/2^+ \rightarrow 1/2^+ + 1^-$ (in units of 10^{12} sec^{-1})

$C_0^+ \rightarrow \Lambda S^+$	0.81	$A^0 \rightarrow \Lambda \bar{K}^{*0}$	0.67
$C_0^+ \rightarrow \Sigma^0 S^+$	0.68	$A^0 \rightarrow \Sigma^0 \bar{K}^{*0}$	2.42
$C_0^+ \rightarrow \Sigma^+ S^0$	0.69	$A^0 \rightarrow \Sigma^+ K^{*-}$	3.78
$C_0^+ \rightarrow \Sigma^+ \omega$	1.84	$A^0 \rightarrow \Xi^0 S^0$	0.37
$C_0^+ \rightarrow \Sigma^+ \varphi$	0.06	$A^0 \rightarrow \Xi^0 \omega$	2.06
$C_0^+ \rightarrow \rho \bar{K}^{*0}$	1.68	$A^0 \rightarrow \Xi^0 \varphi$	0.78
$C_0^+ \rightarrow \Xi^0 K^{*0}$	0.20	$A^0 \rightarrow \Xi^- S^+$	1.69
$A^+ \rightarrow \Sigma^+ \bar{K}^{*0}$	1.22	$T^0 \rightarrow \Xi^0 K^{*0}$	3.60
$A^+ \rightarrow \Xi^0 S^+$	1.66		

Table 11: Partial widths for decays $1/2^+ \rightarrow 3/2^+ + 1^-$ (in units of 10^{12} sec^{-1})

$\Lambda_b^+ \rightarrow \Sigma^{*0} \rho^+$	0.11	$\Lambda^0 \rightarrow \Sigma^{*0} \bar{K}^{*0}$	0.38
$\Lambda_b^+ \rightarrow \Sigma^{*+} \rho^0$	0.11	$\Lambda^0 \rightarrow \Sigma^{*+} K^{*-}$	0.79
$\Lambda_b^+ \rightarrow \Sigma^{*+} \omega$	0.09	$\Lambda^0 \rightarrow \Xi^{*0} \rho^0$	0.26
$\Lambda_b^+ \rightarrow \Sigma^{*+} \varphi$	X	$\Lambda^0 \rightarrow \Xi^{*0} \omega$	0.23
$\Lambda_b^+ \rightarrow \Delta^+ \bar{K}^{*0}$	0.41	$\Lambda^0 \rightarrow \Xi^{*0} \varphi$	X
$\Lambda_b^+ \rightarrow \Delta^{++} K^{*-}$	1.28	$\Lambda^0 \rightarrow \Xi^{*-} \rho^+$	0.51
$\Lambda_b^+ \rightarrow \Xi^{*0} K^{*+}$	X	$\Lambda^0 \rightarrow \Omega^- K^{*+}$	X
$\Lambda^+ \rightarrow \Sigma^{*+} \bar{K}^{*0}$	0.0	$\Lambda^0 \rightarrow \Xi^{*0} \bar{K}^{*0}$	0.13
$\Lambda^+ \rightarrow \Xi^{*0} \rho^+$	0.0	$\Lambda^0 \rightarrow \Omega^- \rho^+$	6.82

Figure Captions

Fig. 1: Quark diagrams for two body decays of C_0^+ . Quark lines are labelled for the specific decay $C_0^+ \rightarrow \Lambda \pi^+ (S^+)$. The appropriate short distance factors are given underneath the diagrams. For neutral final state mesons the short distance factor of (Ia + Ib) is $1/3(2f_+ - f_-)$. Diagrams Ia and Ib are related by Fierz crossing and diagrams IIa and IIb by C-conjugation and crossing.

Fig. 2: Representation of correction term to $\Delta C = 0$ nonleptonic hyperon decays as discussed in [36]. Soft gluon exchange spoils the GIM cancellation of u and c quarks.

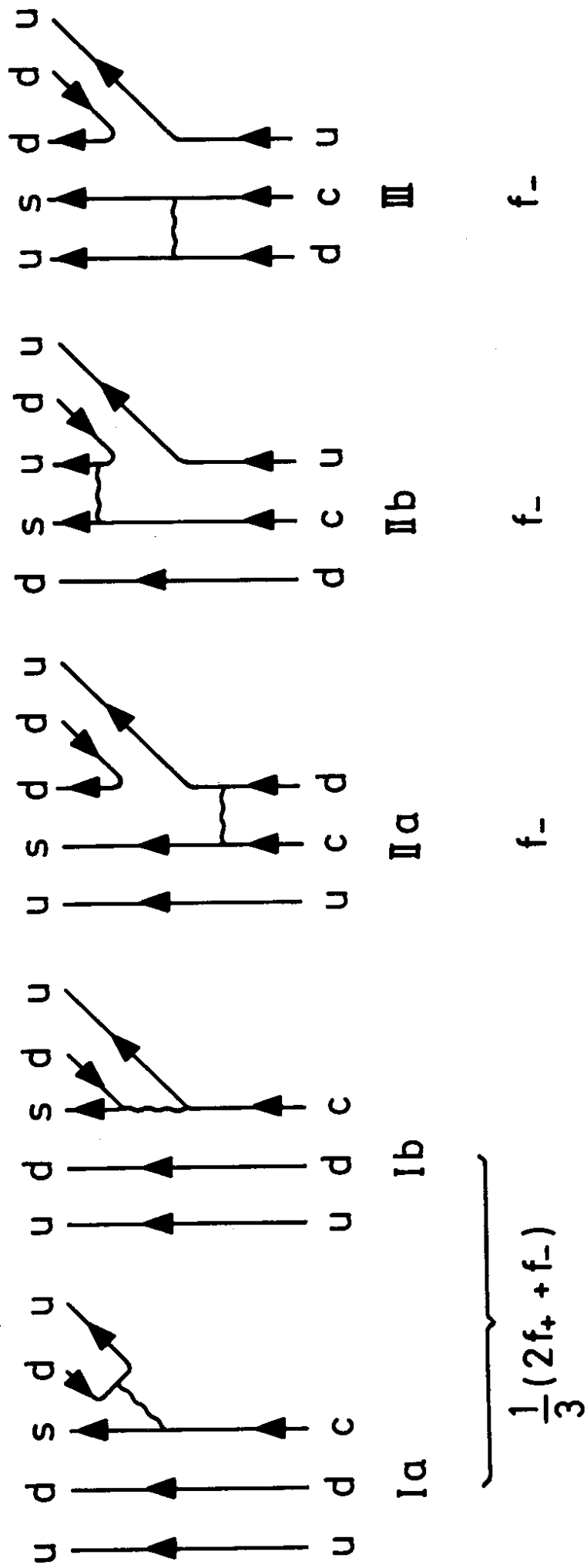


Fig.1

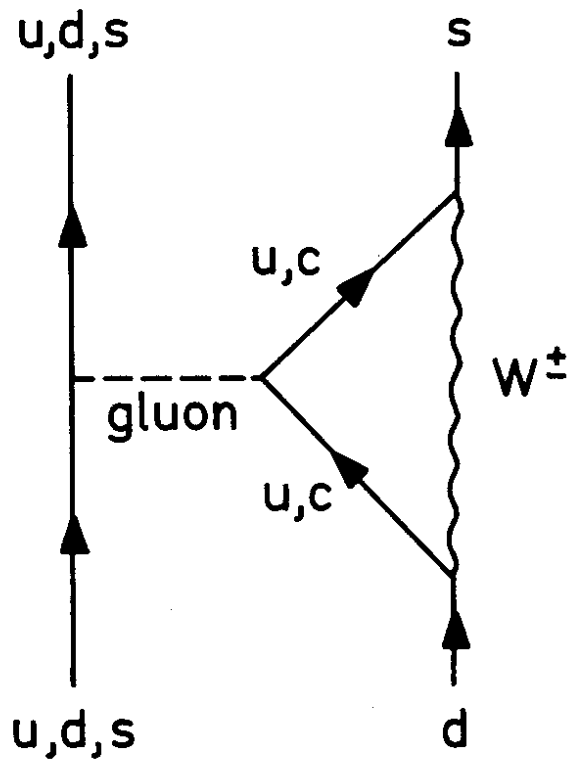


Fig. 2